LF-55

12

THE THORACO-ABDOMINAL SYSTEM'S RESPONSE TO UNDERWATER BLAST

E.R. Fletcher
J.T. Yelverton
D.R. Richmond

September 1976

LOVELACE FOUNDATION
for Medical Education and Research
P.O. Box 5890 Albuquerque, NM 87115

NOTICE

This research was conducted according to the principles enunciated in the "Guide for Laboratory Animal Facilities and Care," prepared by the National Academy of Sciences, National Research Council.

Available from the National Technical Information Service, U. S. Department of Commerce, Springfield, VA 22161

Price: Printed Copy $4.00; Microfiche $3.00.

UNCLASSIFIED
SECURITY CLASSIFICATION OF THIS PAGE (When Data Entered)

REPORT DOCUMENTATION PAGE	READ INSTRUCTIONS BEFORE COMPLETING FORM
1 REPORT NUMBER: LF-55	2 GOVT ACCESSION NO. / 3 RECIPIENT'S CATALOG NUMBER
4 TITLE (and Subtitle): THE THORACO-ABDOMINAL SYSTEM'S RESPONSE TO UNDERWATER BLAST •	5 TYPE OF REPORT & PERIOD COVERED: Final Technical Rept • 1 Jun 74 – 30 Sep 75 • / 6 PERFORMING ORG. REPORT NUMBER
7 AUTHOR(s): E. R. Fletcher, J. T. Yelverton, D. R. Richmond	8 CONTRACT OR GRANT NUMBER(s): N00014-75-C-1079 new
9 PERFORMING ORGANIZATION NAME AND ADDRESS: Lovelace Foundation for Medical Education and Research, Albuquerque, New Mexico 87115	10 PROGRAM ELEMENT PROJECT TASK AREA & WORK UNIT NUMBERS
11 CONTROLLING OFFICE NAME AND ADDRESS: Department of the Navy, Office of Naval Research, Arlington, Virginia 22217	12 REPORT DATE: September 1976 / 13 NUMBER OF PAGES: 58 (1 52 pp)
14 MONITORING AGENCY NAME & ADDRESS (if different from Controlling Office)	15 SECURITY CLASS (of this report): UNCLASSIFIED / 15a DECLASSIFICATION DOWNGRADING SCHEDULE

16 DISTRIBUTION STATEMENT (of this Report)

Approved for public release; distribution unlimited.

17 DISTRIBUTION STATEMENT (of the abstract entered in Block 20, if different from Report)

18 SUPPLEMENTARY NOTES

This work was supported by Office of Naval Research Contract N00014-75-C-1079 with funds provided by the Naval Medical Research and Development Command.

19 KEY WORDS (Continue on reverse side if necessary and identify by block number)

Biophysics of Underwater Blast
Immersion-Blast Injuries
Gastrointestinal-Tract Rupture
Gas-Bubble Oscillation

20 ABSTRACT (Continue on reverse side if necessary and identify by block number)

The purpose of this study was to model the response of the thoraco-abdominal system to underwater-blast waves. The effort focused on the dynamics of submersed gas bubbles because previous studies had shown that most injuries occurred to the gas-containing organs and the immediately adjacent tissues.

Experiments were conducted to obtain data for use as input in the development of a model. Gas-containing balloons, excised organs (swim bladders, gut sections and sheep lungs); excised organs (swim bladders and gut sections) in

DD FORM 1 JAN 73 1473 EDITION OF 1 NOV 65 IS OBSOLETE

UNCLASSIFIED
SECURITY CLASSIFICATION OF THIS PAGE (When Data Entered)

21 pp

gelatin blocks; and whole animals (fish and rats) were viewed with high-speed cameras while being exposed to a shock wave in an underwater test chamber. Overpressure vs time was measured inside the thoraces and abdomens of sheep exposed at either of two depths to underwater blast in a test pond. Both the film and gauge records indicated that the gas bubbles enclosed in the various submersed objects underwent damped oscillations. All rupturing observed in the films occurred while the objects were expanding. In most cases, rupturing began during the first oscillation at a larger volume than the initial one.

In general, the measured frequencies and amplitudes of oscillation were shown to be consistent with the theory for spherical air bubbles undergoing adiabatic changes in free water. Although damping was neglected in this model, the predictions agreed with the measured overpressures and times associated with the first maximum compression of the thoraces of sheep exposed to impulsive loads at a depth of 10 ft. However, all of the peak overpressures measured in the abdomens as well as those measured in the thoraces of sheep near the surface were lower than predicted. Possible reasons for these discrepancies were discussed.

Arguments were presented suggesting that the severity of lung hemorrhage in personnel using scuba gear at various depths below 10 ft might be approximately constant if each diver received an impulsive load proportional to the square root of the hydrostatic pressure at his depth.

LF-55

THE THORACO-ABDOMINAL SYSTEM'S RESPONSE TO UNDERWATER BLAST

September 1976

by

E. R. Fletcher
J. T. Yelverton
D. R. Richmond

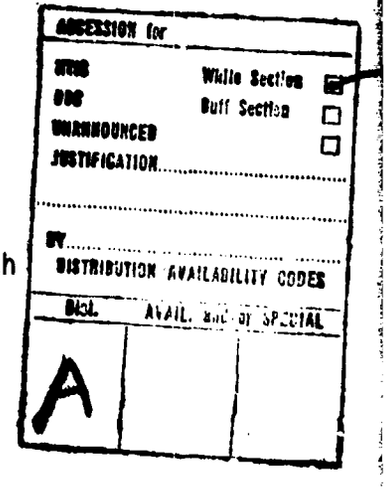

Inhalation Toxicology Research Institute
Lovelace Foundation for Medical Education and Research
P. O. Box 5890, Albuquerque, New Mexico 87115

This work was supported by Office of Naval Research Contract N00014-75-C-1079 with funds provided by the Naval Medical Research and Development Command.

ACKNOWLEDGMENTS

This study was under the direction of R. K. Jones. The technical assistance of E. Damon, K. Saunders, W. Hicks, and R. Hutton is acknowledged. T. Minagawa performed the technical photography and prepared the illustrative material. B. Martinez provided editorial assistance. The final manuscript was processed by N. Barnett.

TABLE OF CONTENTS

LIST OF TABLES

LIST OF FIGURES

THE THORACO-ABDOMINAL SYSTEM'S RESPONSE TO UNDERWATER BLAST

by

E. R. Fletcher, J. T. Yelverton and D. R. Richmond

I. INTRODUCTION

A. *Objectives*

The objectives of this study were (a) to submerse various gas-containing test objects, including excised lungs and isolated sections of gastrointestinal tract, in an underwater-test chamber where they could be viewed with high-speed cameras while being exposed to a shock wave; (b) to measure overpressure vs time inside the thoraces and abdomens of sheep exposed at either of two depths to a shock wave in a test pond; and (c) to use the results of these studies to model the response of the thoraco-abdominal system to underwater-blast waves.

B. *Background*

In 1969, the Lovelace Foundation began a series of studies to establish the probability of injury and mortality in animals exposed to underwater blast (1-3). As in earlier studies, most of the injuries occurred to the gas-containing organs (lungs, gastroenteric tract and ears) and the immediately adjacent tissues. The injury and mortality levels were determined to be functions of the overpressure impulse of the incident shock wave.

In 1973, a study was begun to provide information on damage mechanisms associated with gas bubbles in the G.I. tract. Thirteen-cm-long sections of small intestine or rectum were remo ed from sheep and filled with water. Air bubbles of various volumes (0.1 to 8.0 cm^3) were injected into the sections which were then exposed to a blast wave in free water. The results suggested that perforation of the G.I. tract is related to magnitude of the impulse, volume of the bubble and wall thickness of the organ surrounding the bubble. The lower line in Figure 1 approximates the data for sections of small intestine in free water.

In 1974, experiments were conducted to determine the underwater-blast impulse levels required to perforate the G.I. tract containing a known bubble volume while inside an anesthetized animal. In some experiments, 13-cm lengths of small intestine were tied off in place and injected with air bubble volumes

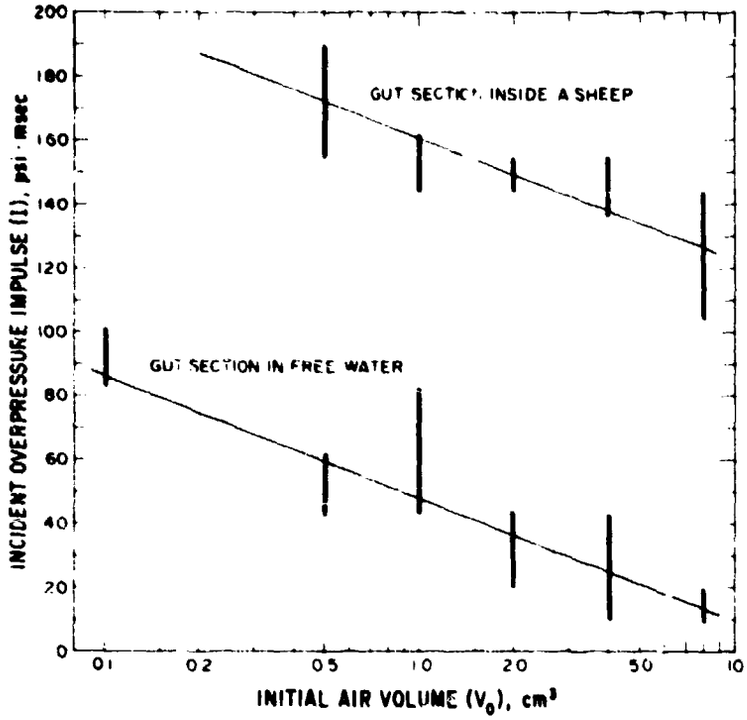

Figure 1. Fifty percent probability that an underwater blast will rupture a tied-off section of sheep small intestine containing an air pocket. Note that, for a given air volume, the impulse required to rupture a gut section inside a sheep was approximately 113 psi·msec greater than the impulse required to rupture a similar section in free water.

from 0.5 to 8.0 cm^3. In other experiments, an intestinal section from one sheep was transplanted into the abdominal cavity of another. Because no significant differences were noted, the data for transplanted and in-place sections were combined. The results were similar to those for sections exposed in free water; however, for a given bubble volume, the impulse required to rupture a section inside a sheep was approximately 113 psi·msec greater than the impulse required to rupture a similar section in free water (Figure 1).

The above studies established the approximate impulse levels required to produce rupture and demonstrated the profound influence of the presence of the body surrounding the gas-containing organ. However, little was learned about the dynamics of enclosed gas bubbles during their exposure to blast or about the mechanisms of damage to the surrounding tissues. It was anticipated that such information could be derived from motion pictures of gas-containing excised organs and from overpressure vs time records obtained with gauges inside the thoraces and abdomens of animals during their exposure to underwater blast. The technical feasibility of measuring thoracic pressures inside animals has been demonstrated in earlier airblast studies (4). Records from these studies were used in developing a thoraco-abdominal model for airblast. This model has been useful in explaining many observed phenomena and in predicting injury levels for untested experimental geometries (4). A model for underwater blast could be similarly useful, particularly in predicting injury to personnel at greater depths than have been tested extensively.

II. PROCEDURE

A. *Chamber Tests*

The test chamber consisted of a cylindrical 3/4-inch-thick steel tank (63-inch length, 41-inch diameter) whose axis paralleled the ground. The test object was positioned at the center of the tank using a 1/4-inch steel rod. The tank was filled to a maximum depth of 33 inches, with the center of the object being 12.5 inches below the surface. The atmospheric pressure at the test chamber was 12.0 psi, giving a hydrostatic pressure of 12.45 psi at the test object. The charge (an E-99 blasting cap from DuPont, 0.875 gm of explosive) was mounted on a 1/4-inch steel rod and positioned either at the same depth or directly

below the test object. In all cases, the charge was 18 inches from the object, 2.5 inches from the curved wall and 31.5 inches from either end of the cylinder. A manhole (17-inch diameter) which was centered on the top of the tank remained open during the tests. A Plexiglas viewing port (24-inch diameter, 2-inch thickness) was centered on either end of the chamber.

A total of 52 objects were exposed in 42 tests conducted in the chamber. The test objects and the initial gas volumes are given in Table 1. Except for the balloons, the initial volumes were measured before the objects were submersed, but this made little difference because the atmospheric and hydrostatic pressures were approximately equal.

1. *Balloons*

A total of eight tests were conducted with ordinary balloons that were approximately spherical in shape. Five small-sized balloons had initial air volumes ranging from 91 to 695 cm^3, whereas they could have been inflated slowly to over 2500 cm^3 before rupturing. Three large-sized balloons had initial air volumes ranging from 2290 to 2370 cm^3, whereas they could have been inflated slowly to over 15000 cm^3 before rupturing. Because they were so softly inflated, the initial pressure in the balloons was approximately equal to the hydrostatic pressure at the depth of the balloons (i.e., 12.45 psi).

2. *Swim Bladders*

The four swim bladders used in this study were excised from carp. The total volume of each of the two-chambered bladders is given in Table 1. Two of the swim bladders were encased in the centers of two 4 x 7.5 x 18-cm blocks of 20% (by weight) gelatin used to simulate tissue. Each block had a mass of approximately 500 gm.

3. *Gut Sections*

Twenty-four 13-cm long sections of small intestine from sheep were exposed, singly or in groups of three, in the test chamber. The ends were tied off prior to filling each section with water and an air bubble with a volume of 0.1, 0.5, 1, 2, 4 or 8 cm^3. Two of the gut sections were encased in gelatin blocks of similar size and composition to those used with the swim bladders.

TABLE 1

OSCILLATION OF GAS BUBBLES IN OBJECTS EXPOSED

TO SHOCK WAVES IN THE UNDERWATER TEST CHAMBER*

Test Number	Test Object	Initial Volume (V_o), cm^3	Values Apply to First Oscillation				Volume at Rupture (V_r), cm^3	Time to Rupture (T_r), msec	Oscillation Frequency ($f \approx 1000/\tau$) cycles/sec
			Minimum Volume (V_c), cm^3	Time to V_c (T_c), msec	Maximum Volume (V_e), cm^3	Time to V_e (T_e), msec			
1	Balloon	91	5.6	1.0	580	5.9	381	3.4	85
2	Balloon	275	67	1.9	697	7.7	375[j]	43.2[j]	74
3	Balloon	298	54	1.9	1010	9.9	645	5.5	75
4	Balloon	298	64	1.9	984	8.2	493	5.1	76
5	Balloon	695	212	2.2	1620	10.9	1070	6.3	58
6	Balloon	2290	942	4.4	4540	20.7	1570[j]	75.3[j]	33
7	Balloon	2370	1090	4.1	5080	17.2	301[j]	47.6[j]	31
8	Balloon	2370	-	-	-	-	- [j]	~48[j]	-
9	Swim Bladder[d]	17	5.0	0.6	43	2.9	-	1.0	155
10	Swim Bladder[d]	39	3.6	0.8	204	4.2	-	1.9	132
11	Swim Bladder in Gelatin[d,e]	30	9	0.5	-	2.3	-	~1.4	170
12	Swim Bladder in Gelatin[d,e]	36	9	0.5	77	3.3	-	~0.7	179
13	Gut Section[f]	0.1	-	-	-	-	No Rupture		-
14	Gut Section[f]	0.5	-	-	-	-	No Rupture		-
15	Gut Section[f]	1.0	-	-	-	-	No Rupture		-
16[a]	Gut Section[f]	0.1	-	-	-	-	No Rupture		-
16[b]	Gut Section[f]	0.5	-	-	-	-	No Rupture		-
16[c]	Gut Section[f]	1.0	-	-	-	-	No Rupture		404
17[a]	Gut Section[f]	0.1	-	-	-	-	No Rupture		-
17[b]	Gut Section[f]	0.5	-	-	-	-	No Rupture		766
17[c]	Gut Section[f]	1.0	-	-	-	0.6	No Rupture		583
18	Gut Section[f]	2.0	-	-	-	-	-	-	-
19	Gut Section[f]	2.0	-	-	-	3.1	-	1.2	332
20	Gut Section[f]	4.0	-	-	-	3.1	-	1.4	246
21	Gut Section[f]	8.0	-	0.5	-	3.6	-	3.0	203
22[a]	Gut Section[f]	2.0	-	-	-	1.9	-	-	335
22[b]	Gut Section[f]	4.0	-	-	-	3.1	-	-	242
22[c]	Gut Section[f]	8.0	-	~0.3	-	3.7	-	1.6	177
23[a]	Gut Section[f]	2.0	-	-	-	1.9	No Rupture		336
23[b]	Gut Section[f]	4.0	-	-	-	-	No Rupture		-
23[c]	Gut Section[f]	8.0	-	0.5	-	2.6	-	1.8	250
24[a]	Gut Section[f]	2.0	-	-	-	-	No Rupture		-
24[b]	Gut Section[f]	4.0	-	-	-	-	No Rupture		-
24[c]	Gut Section[f]	8.0	-	-	-	-	-	-	-
25	Gut Section in Gelatin[e,f]	2.0	-	-	-	1.9	No Rupture		471
26	Gut Section in Gelatin[e,f]	8.0	-	~0.2	-	2.0	No Rupture		292
27	Left Lung of Sheep[g]	~500	-	2.2	-	9.9	-	-	56
28	Right Lung of Sheep[g]	~700	-	3.4	-	13.6	-	-	42
29	Goldfish, 39 gm	~3	-	-	-	-	-	-	-
30	Goldfish, 57 gm	~4	-	-	-	-	-	-	-
31	Goldfish, 73 gm	~5	-	-	-	-	-	-	-
32	Goldfish, 107 gm	~7	-	-	-	-	-	-	-
33	Goldfish, 133 gm	~9	-	-	-	-	-	-	-
34	Goldfish, 273 gm	~18	-	-	-	-	-	-	-
35	Goldfish, 382 gm	~25	-	-	-	-	-	-	-

An explanation of the symbols is given at the end of the table.

TABLE 1 (Continued)

OSCILLATION OF GAS BUBBLES IN OBJECTS EXPOSED

TO SHOCK WAVES IN THE UNDERWATER TEST CHAMBER*

Test Number	Test Object	Initial Volume (V_o), cm^3	Values Apply to First Oscillation				Volume at Rupture (V_r), cm^3	Time to Rupture (T_r), msec	Oscillation Frequency ($f \cong 1000/\tau$) cycles/sec
			Minimum Volume (V_c), cm^3	Time to V_c (T_c), msec	Maximum Volume (V_e), cm^3	Time to V_e (T_e), msec			
36	Rat,[i] 570 gm	~6	-	-	-	-	-	-	-
37	Rat,[i] 611 gm	~6	-	-	-	-	-	-	-
38	Rat,[i] 627 gm	~6	-	-	-	-	-	-	-
39	Rat,[j] 629 gm	~6	-	-	-	-	-	-	-
40	Rat,[h] 616 gm	~6	-	-	-	-	-	-	196
41	Rat,[h] 622 gm	~6	-	-	-	-	-	-	233
42	Rat,[h] 651 gm	~6	-	-	-	-	-	-	208

* An E-99 blasting cap was detonated 18 inches from the test objects which were submersed to a depth of 12.5 inches. See text for details of the experimental arrangement.

All volumes refer to air volumes.

\- Not measureable from film record.

~ Value only approximate.

a, b, c } One of three objects exposed on a single test.

d The swim bladders were excised from carp.

e Object in a 4x7.5x18-cm block of 20% (by weight) gelatin with a mass of approximately 500 gm.

f The gut sections were 13-cm-long sections of sheep small intestine filled with water and an air bubble of the indicated volume.

g The lungs were excised from a 39-kg sheep.

h Shaved rat; tracheal ligature used; thru & thru enema given to eliminate abdominal gas.

i Shaved rat; no tracheal ligature used; no enema given.

j Balloon aspherical at time of rupture.

4. *Sheep Lungs*

The excised left and right lungs of a 39-kg sheep were clamped off before being exposed to underwater blast on separate tests. The lungs contained the functional residual volume of air.

5. *Fish*

Seven goldfish (39 to 382 gm) were anesthetized (Ethyl Carbamate) prior to their exposure in the chamber while being held in place with strands of suture. The initial gas volumes of the swim bladders were estimated from the body mass using data obtained earlier with similar goldfish.

6. *Rats*

Seven freshly-sacrificed rats (570 to 651 gm) were subjected to underwater blast in the test chamber. The rats had been shaved and dipped in a wetting agent in order to decrease the possibility of air bubbles' being trapped next to the body. Such bubbles would reduce the quality of the motion pictures to be taken and they might affect the animals' response to underwater blast.

It was noted that a small amount of gas escaped from the tracheas as the first four rats exposed were lowered into the water. Attempts to determine the oscillation frequency of the thorax by analyzing the motion pictures of these four animals were complicated by the presence of gas pockets in the abdomen which were also oscillating, but at different frequencies. These problems were eliminated on the last three rats tested by using tracheal ligation to keep gas from escaping and a through-and-through enema to eliminate abdominal gas. The volume of gas in the lungs was estimated from the body mass.

7. *Motion Pictures*

A Fastax camera (Wollensak Optical Company) operating at an average of 4100 frames per second was used to view the objects during their exposure to underwater shock in the test chamber. Lighting was supplied by six 650-watt flood lights located in the porthole at the top of the tank and one long-duration flashbulb (equivalent to an 1100-watt flood light for 1.75 sec) located in the water approximately 12 inches from the test object.

8. *Incident Shock Wave*

The principal force oscillating the gas bubbles in the test chamber was the direct shock wave from the blasting cap plus the complex reflection of that wave against the curved, steel wall of the tank. The main component of the second wave had to travel approximately 5 inches farther than the first wave in order to reach the test object. The time interval corresponding to the effective durations of these two waves plus the spacing between them was short compared to the oscillation period of any of the objects tested such that, in all cases, the load could be regarded as impulsive (i.e., the response of the objects should be a function of only the total impulse of the two waves). The short durations made it unfeasible to accurately measure the impulses with the available gauges. However, in unpublished experiments previously conducted at the Lovelace Foundation, impulses were measured at ranges from 9 to 36 ft in free water, and it was possible to scale those to the 1.5-ft range for the experiments in the test chamber. On the basis of this scaling, a total impulse between 29 and 52 psi·msec was predicted. It was anticipated that the actual impulse could be estimated more exactly (a) by comparing the observed balloon oscillations with the theoretical predictions and (b) by comparing the observed frequency of gut-section rupture with the earlier data (Figure 1).

B. *Pond Tests*

The sheep were exposed to underwater blast in a test pond which measured 220 by 150 ft at the surface and was 30 ft deep over its 100- by 30-ft central portion. The pond is described in Reference 1. A 1- or 8-lb bare sphere of cast Pentolite was detonated at a depth of either 1 or 10 ft at various ranges from the animals. Previous tests had indicated that, for the present experimental arrangement, bottom reflections would be negligible. The atmospheric pressure at the test pond was 12.0 psi.

1. *Sheep*

Seven sheared sheep (36-43 kg) were exposed to a total of 45 detonations in the test pond (Table 2). Although some of the animals were used on as many as eight tests, no change was noted in the internal overpressure records as a result of the multiple exposures. Nonetheless, in an attempt to reduce the possibility of the early tests disturbing the gas pockets in such a way as to

TABLE 2

PRESSURE OSCILLATIONS INSIDE SHEEP EXPOSED TO SHOCK WAVES IN THE TEST CHAMBER

					Incident Shock Wave[a]					Internal Pressure Wave[b]									
										Maximum Overpressure in Each of First Seven Oscillations, psi									
Test Number	Animal Number	Charge Mass (W), lb	Gauge Location	Depth of Gauge (D_g), ft	Slant Range (S), ft	Peak Over-Pressure (P_1), psi	Surface Cut-Off Time (T_1), msec	Over-Pressure Impulse (I), psi-msec	Decay Time Constant (θ), msec	P_c	P_{c2}	P_{c3}	P_{c4}	P_{c5}	P_{c6}	P_{c7}	Time to P_c (T_c), msec	Minimum Overpressure in First Oscillation (P_e), psi	Oscillation Frequency (f = 1000/τ) cycles/sec
1	1	1	Thorax	1	27.0	521	.154	45.9	.124	-	-	-	-	-	-	-	-	-	-
			Abdomen	2	26.7	528	.307	59.8	.124	-	-	-	-	-	-	-	-	-	-
2	1	1	Thorax	1	27.0	521	.154	45.9	.124	10.0	-	-	-	-	-	-	3.55	-	-
			Abdomen	2	26.7	528	.307	59.8	.124	40.7	-	-	-	-	-	-	1.07	-	-
3	2	1	Thorax	1	63.0	200	.0667	10.8	.149	1.8	-	-	-	-	-	-	2.82	-	-
			Abdomen	2	62.9	201	.133	17.7	.149	15.6	15.6	5.9	5.9	1.7	1.7	1.7	0.94	-6.2	129
4	2	1	Thorax	1	63.0	200	.0667	10.8	.149	-	-	-	-	-	-	-	3.72	-	-
			Abdomen	2	62.9	201	.133	17.7	.149	16.6	14.5	6.9	6.9	1.7	1.7	1.7	0.74	-6.6	124
5	2	1	Thorax	1	42.0	316	.0997	22.4	.136	4.3	-	-	-	-	-	-	3.44	-	-
			Abdomen	2	41.8	318	.199	33.3	.136	41.3	54.9	6.6	6.6	-	-	-	0.95	-9.5	110
6	2	1	Thorax	1	42.0	316	.0997	22.4	.136	4.5	-	-	-	-	-	-	3.03	-	-
			Abdomen	2	41.8	318	.199	33.3	.136	41.7	56.7	12.1	6.6	-	-	-	1.22	-10.2	107
7	2	1	Thorax	1	27.0	521	.154	45.9	.124	9.2	-	-	-	-	-	-	2.67	-	49.8
			Abdomen	2	26.7	528	.307	59.8	.124	102	80.0	12.8	3.2	3.2	-	-	0.80	-12.9*	99.5
8	2	1	Thorax	1	16.0	942	.254	93.5	.110	26.3	14.6	-	-	-	-	-	1.90	-	51.9
			Abdomen	2	15.5	979	.506	106	.110	202	77.2	28.4	-	-	-	-	0.44	-12.9*	107
9	2	1	Thorax	1	16.0	942	.254	93.5	.110	24.0	16.9	-	-	-	-	-	1.97	-	49.8
			Abdomen	2	15.5	979	.506	106	.110	288	-	-	-	-	-	-	0.37	-12.9*	108
10	2	1	Thorax	1	16.0	942	.254	93.5	.110	-	-	-	-	-	-	-	-	-	-
			Abdomen	2	15.5	979	.506	106	.110	379	-	-	-	-	-	-	0.27	-12.9*	111
11	3	1	Thorax	1	63.0	200	.0667	10.8	.149	-	-	-	-	-	-	-	-	-	-
			Abdomen	2	62.9	201	.133	17.7	.149	17.8	-	-	-	-	-	-	0.56	-6.3	135
12	3	1	Thorax	1	42.0	316	.0997	22.4	.136	-	-	-	-	-	-	-	-	-	-
			Abdomen	2	41.8	318	.199	33.3	.136	39.2	-	-	-	-	-	-	0.42	-	156
13	3	1	Thorax	1	27.0	521	.154	45.9	.124	7.6	-	-	-	-	-	-	3.75	-	43.1
			Abdomen	2	26.7	528	.307	59.8	.124	81.2	38.0	-	-	-	-	-	0.42	-	153
14	3	1	Thorax	1	16.0	942	.254	93.5	.110	-	-	-	-	-	-	-	-	-	-
			Abdomen	2	15.5	979	.506	106	.110	271	-	-	-	-	-	-	0.29	-12.9*	-
15	3	1	Thorax	1	11.0	1300	.329	129	.104	63.3	28.5	-	-	-	-	-	1.39	-	48.7
			Abdomen	2	11.3	1400	.657	143	.102	414	31.4	20.0	-	-	-	-	0.35	-12.9*	108
16	3	1	Thorax	1	12.0	1300	.329	129	.104	60.3	-	-	-	-	-	-	2.72	-	-
			Abdomen	2	11.3	1400	.657	143	.102	449	31.9	31.9	-	-	-	-	0.21	-12.9*	121

An explanation of the symbols is given at the end of the table.

TABLE 2 (Continued)

PRESSURE OSCILLATIONS INSIDE SHEEP EXPOSED TO SHOCK WAVES IN THE TEST CHAMBER

Test Number	Animal Number	Charge Mass (W), lb	Gauge Location	Depth of Gauge (Dg), ft	Incident Shock Wave[a]					Internal Pressure Wave[b]									
					Slant Range (S), ft	Peak Overpressure (Pi), psi	Surface Cut-Off Time (Ti), msec	Overpressure Impulse (I), psi·msec	Decay Time Constant (θ), msec	Maximum Overpressure in Each of First Seven Oscillations, psi							Time to P_c (T_c), msec	Minimum Overpressure in First Oscillation (P_e), psi	Oscillation Frequency (f = 1000/τ) cycles/sec
										P_c	P_{c2}	P_{c3}	P_{c4}	P_{c5}	P_{c6}	P_{c7}			
17	4	8	Thorax	1	69.0	395	0609	21.5	.261	-	-	-	-	-	-	-	-	-	-
			Abdomen	2	68.9	396	.122	38.5	.261	32.0	13.3	13.3	-	-	-	-	0.77	-	193
18	4	8	Thorax	1	69.0	395	.0609	21.5	.261	-	-	-	-	-	-	-	-	-	-
			Abdomen	2	68.9	396	.122	38.5	.261	52.3	8.8	8.8	-	-	-	-	0.61	-	189
19	4	8	Thorax	1	48.0	595	.0873	43.6	.241	-	-	-	-	-	-	-	-	-	-
			Abdomen	2	47.8	598	.174	74.3	.241	99.0	-	-	-	-	-	-	0.32	-12.9*	185
20	4	8	Thorax	1	32.0	942	.130	92.7	.221	-	-	-	-	-	-	-	-	-	-
			Abdomen	2	31.7	951	.260	145	.220	266	-	-	-	-	-	-	0.23	-12.9*	-
21	4	8	Thorax	1	26.0	1190	.160	133	.211	-	-	-	-	-	-	-	-	-	-
			Abdomen	2	25.7	1210	.319	198	.210	326	-	-	-	-	-	-	0.22	-12.9*	-
22	4	8	Thorax	10	69.0	395	.598	92.8	.261	-	-	-	-	-	-	-	-	-	-
			Abdomen	11	69.0	395	.656	94.9	.261	98.8	-	-	-	-	-	-	0.46	-12.9*	-
23	4	8	Thorax	10	52.0	544	.782	128	.246	-	-	-	-	-	-	-	-	-	-
			Abdomen	11	52.0	544	.857	130	.246	117	-	-	-	-	-	-	0.46	-12.9*	-
24	5	1	Thorax	10	84.0	145	.494	22.0	.159	5.7	-	-	-	-	-	-	3.08	-	-
			Abdomen	11	84.0	145	.543	22.2	.159	14.7	36.8	36.8	8.0	3.4	3.4	-	0.99	-10.7	119
25	5	1	Thorax	10	84.0	145	.494	22.0	.159	5.2	-	-	-	-	-	-	2.80	-	-
			Abdomen	11	84.0	145	.543	22.2	.159	22.3	30.6	30.6	7.7	7.7	7.7	-	0.85	-9.8	121
26	5	1	Thorax	10	47.0	279	.859	38.9	.140	18.8	-	-	-	-	-	-	2.87	-	54.0
			Abdomen	11	47.0	279	.940	38.9	.140	41.1	26.4	26.4	4.1	4.1	4.1	-	0.64	-11.2	121
27	5	1	Thorax	10	47.0	279	.859	38.9	.140	19.1	-	-	-	-	-	-	3.36	-	57.6
			Abdomen	11	47.0	279	.940	38.9	.140	38.6	19.6	19.6	4.8	4.8	4.8	-	0.64	-11.9	121
28	5	1	Thorax	10	26.0	544	1.43	66.8	.123	48.2	-	-	-	-	-	-	2.80	-	54.1
			Abdomen	11	26.0	543	1.56	66.8	.123	89.2	19.2	19.2	9.6	9.6	9.6	-	0.37	-13.7	123
29	5	1	Thorax	10	26.0	544	1.43	66.8	.123	68.5	30.0	13.2	-	-	-	-	2.52	-	55.2
			Abdomen	11	26.0	543	1.56	66.8	.123	151	21.9	21.9	11.0	11.0	-	-	0.37	-16.8*	124
30	5	1	Thorax	10	19.0	775	1.81	88.9	.115	112	44.8	-	-	-	-	-	1.83	-	52.0
			Abdomen	11	19.0	774	1.96	88.8	.115	268	24.7	24.7	17.6	17.6	-	-	0.37	-16.8*	127
31	5	1	Thorax	10	19.0	775	1.81	88.9	.115	99.8	54.9	-	-	-	-	-	2.15	-	53.4
			Abdomen	11	19.0	774	1.96	88.8	.115	339	33.9	22.6	22.6	22.6	-	-	0.28	-16.8*	129
32	6	1	Thorax	10	84.0	145	.494	22.0	.159	2.4	-	-	-	-	-	-	4.87	-	-
			Abdomen	11	84.0	145	.543	22.2	.159	13.6	12.9	12.9	12.9	4.0	4.0	4.0	0.62	-7.2	143

An explanation of the symbols is given at the end of the table.

TABLE 2 (Continued)

PRESSURE OSCILLATIONS INSIDE SHEEP EXPOSED TO SHOCK WAVES

IN THE TEST CHAMBER

					Incident Shock Wave[a]					Internal Pressure Wave[b]									
Test Number	Animal Number	Charge Mass (W), lb	Gauge Location	Depth of Gauge (D_g), ft	Slant Range (S), ft	Peak Overpressure (P_i), psi	Surface Cut-Off Time (T_i), msec	Overpressure Impulse (I), psi·msec	Decay Time Constant (θ), msec	Maximum Overpressure in Each of First Seven Oscillations, psi							Time to P_c (T_c), msec	Minimum Overpressure in First Oscillation (P_e), psi	Oscillation Frequency (f = 1000/τ) cycles/sec
										P_c	P_{c2}	P_{c3}	P_{c4}	P_{c5}	P_{c6}	P_{c7}			
33	6	1	Thorax	10	64.0	145	.494	22.0	.159	6.4	-	-	-	-	-	-	5.31	-	-
			Abdomen	11	84.0	145	.543	22.2	.159	20.6	12.7	12.7	9.4	2.9	2.9	2.9	0.76	-8.3	144
34	6	1	Thorax	10	47.0	279	.859	38.9	.140	16.5	-	-	-	-	-	-	4.50	-	-
			Abdomen	11	47.0	279	.941	38.9	.140	58.5	30.8	6.5	6.5	-	-	-	0.69	-	146
35	6	1	Thorax	10	47.0	279	.859	38.9	.140	17.6	-	-	-	-	-	-	4.57	-	45.8
			Abdomen	11	47.0	279	.941	38.9	.140	55.7	13.6	-	-	-	-	-	0.55	-	146
36	6	1	Thorax	10	26.0	544	1.43	66.8	.123	39.0	-	-	-	-	-	-	4.43	-	46.3
			Abdomen	11	26.0	543	1.56	66.8	.123	109	-	-	-	-	-	-	0.27	-16.8*	149
37	6	1	Thorax	10	26.0	543	1.43	66.8	.123	29.4	26.2	-	-	-	-	-	4.77	-	45.8
			Abdomen	11	26.0	543	1.56	66.8	.123	126	-	-	-	-	-	-	0.27	-16.8*	149
38	6	1	Thorax	10	19.0	775	1.81	88.9	.115	120	51.6	-	-	-	-	-	2.90	-	45.9
			Abdomen	11	19.0	774	1.96	88.8	.115	184	-	-	-	-	-	-	0.27	-16.8*	153
39	6	1	Thorax	10	19.0	775	1.81	88.9	.115	89.6	58.5	21.9	-	-	-	-	2.69	-	45.7
			Abdomen	11	19.0	774	1.96	88.8	.115	208	-	-	-	-	-	-	0.27	-16.8*	149
40	7	8	Thorax	10	69.0	395	.598	92.8	.261	58.2	-	-	-	-	-	-	1.59	-	41.2
			Abdomen	11	69.0	395	.656	94.9	.261	82.9	47.8	47.8	10.7	10.7	-	-	0.76	-12.2	102
41	7	8	Thorax	10	69.0	395	.598	92.8	.261	47.8	-	-	-	-	-	-	1.56	-	42.1
			Abdomen	11	69.0	395	.656	94.9	.261	145	58.1	58.1	-	-	-	-	0.62	-16.8*	99.6
42	7	8	Thorax	10	52.0	544	.782	128	.246	73.2	54.9	-	-	-	-	-	1.51	-	40.8
			Abdomen	11	52.0	544	.857	130	.246	242	70.6	70.6	-	-	-	-	0.55	-16.8*	105
43	7	8	Thorax	10	52.0	544	.782	128	.246	67.9	41.0	-	-	-	-	-	1.31	-	40.2
			Abdomen	11	52.0	544	.857	130	.246	240	37.0	37.0	-	-	-	-	0.48	-16.8*	104
44	7	8	Thorax	10	52.0	544	.782	128	.246	61.9	-	-	-	-	-	-	1.37	-	-
			Abdomen	11	52.0	544	.857	130	.246	186	65.2	65.2	-	-	-	-	0.55	-16.8*	96.5
45	7	8	Thorax	10	52.0	544	.782	128	.246	52.4	-	-	-	-	-	-	1.17	-	-
			Abdomen	11	52.0	544	.857	130	.246	202	62.3	62.3	-	-	-	-	0.48	-16.8*	96.1

- Not measureable from gauge record.
* Although an accurate measurement could not be obtained from the gauge record, P_e was approximately equal to the indicated $-P_o$, the negative of the hydrostatic pressure.
[a] Calculated values given.
[b] Measured values given.

modify the internal overpressures recorded on the later tests, multiple exposures were conducted in the order of increasing dose (i.e., incident impulse). The volume of the gas in the lungs was estimated from the body mass.

Three anesthetized (Sodium Pentobarbital) sheep were exposed at the surface of the water, three freshly sacrificed sheep were exposed at a 10-ft depth and one animal was exposed at both depths. The anesthetized animals died after the first few exposures, but this appeared to have no significant effect on the internal overpressures recorded on the subsequent exposures. All of the animals were mounted vertically in the water with their long axes perpendicular to the surface. The mounting apparatus is described in reference 2. The animals at the surface had their heads above water and their shoulders just below the surface. The xiphisternum was at a depth of approximately 1 ft. A plastic bag was closed tightly over the mouth and nostrils of each sheep exposed with its xiphisternum at a depth of 10 ft. This prevented water from entering the animal while it was submersed.

2. *Internal Overpressures*

The overpressures inside the sheep were measured using two modified Type B gauges which were developed at the Naval Surface Weapons Center. The sensing element of the gauge consisted of four 1/4-inch-diameter tourmaline discs mounted in a Tygon® tube filled with silicone oil (Dow-Corning No. 200 dielectric oil). One gauge was inserted in the esophagus to the level of the xiphisternum; when the animal was in the water, the gauge was at a depth of either 1 or 10 ft corresponding to a hydrostatic pressure of either 12.43 or 16.33 psi, respectively. The other gauge was inserted approximately 7 inches into the rectum; it was at a depth of either 2 or 11 ft corresponding to a hydrostatic pressure of either 12.87 or 16.77 psi, respectively. The output from each gauge was recorded on a dual-beam oscilloscope at sweep rates of both 1 and 5 msec/cm.

3. *Incident Shock Wave*

Two additional modified Type B gauges were located in free water at the same ranges and depths as the two gauges inside each sheep. To assure that the presence of the animal would not modify the shock wave incident on an external gauge, a separation distance of 12 ft was maintained throughout the tests.

As in the case of the objects exposed in the experimental chamber, the durations of the incident shock waves were short compared to the oscillation periods of the sheep thoraces and abdomens; therefore the load could be considered as impulsive in all cases. Ranges were chosen to give impulses to the thorax of from 11 to 133 psi·msec and impulses to the abdomen of from 18 to 198 psi·msec. Previous studies (1-2) indicate that 10 psi·msec should result in threshold lung hemorrhage, whereas impulses of approximately 100 psi·msec are required to produce gut ruptures (Table 1).

III. RESULTS AND DISCUSSION

A. *Chamber Tests*

1. *Damage to Test Objects*

The test objects received the following damage during their exposure in the chamber. All eight balloons and both chambers of all four excised swim bladders (two of which were in gelatin) were ruptured. None of the nine gut sections in free water with 0.1, 0.5 or 1 cm^3 of air ruptured, whereas three of the five sections with 2 cm^3, two of the four sections with 4 cm^3, and all four sections with 8 cm^3 ruptured. Neither of the gut sections (2 and 8 cm^3 of air) in gelatin ruptured. Both excised sheep lungs had deep lacerations and multiple blebs. All seven goldfish sustained multiple injuries, including ruptured swim bladders, resulting in lethality. The seven rats had moderate to extensive lung hemorrhage and multiple intra-abdominal lesions including gut ruptures and liver lacerations.

2. *Motion Pictures*

In general, the quality of the motion pictures from the test chamber was good. However, some of the test objects were obscured for a few frames when cavitation occurred at the interface between the water and the Plexiglas viewing port. The films were analyzed to determine the maximum and minimum bubble volumes and their times of occurrence for each oscillation. Some of the balloons developed very aspherical shapes while oscillating prior to rupturing. The volume and time of rupture were also determined. In all cases, the volume was estimated from the projected area measured with a planimeter. For the smaller volumes, it was necessary to interpolate between frames in order to obtain

accurate minimum volumes. The volumes and times associated with the first oscillation and rupture are given in Table 1, where the subscript "o" refers to initial conditions, "c" refers to conditions at maximum compression (i.e., minimum volume), "e" refers to conditions at maximum expansion (i.e., maximum volume) and "r" refers to conditions at rupture.

Figures 2 and 3 show the oscillations of the balloons on test numbers 5 and 2, respectively. The radius "R" of a spherical air bubble equivalent to the measured volume, regardless of its actual shape, has been plotted against time. As these figures suggest, oscillation frequencies could be determined but rates of damping could not. Although the bubble motion did eventually damp out, the process was complicated by oscillations of the explosion bubble and the fact that the air bubble being tested appeared larger after rupture than before. The latter effect can be seen in Figures 2 and 3 where, in both cases, the oscillations center approximately around the initial radius prior to rupture and a larger radius after rupture. Nonetheless, the rupturing never noticeably changed the frequency of oscillation, probably due to the fact that the balloons and other objects were softly inflated initially.

Oscillation frequencies could be determined for some of the filmed objects even though the gas bubble could not be seen directly, and therefore maximum and minimum volumes could not be measured. These frequencies are also given in Table 1.

3. *Incident Shock Wave*

As discussed earlier, the effective overpressure impulse incident on the objects in the test chamber was predicted to be between 29 and 52 psi·msec. In a later section, comparisons between observed balloon oscillations and theoretical predictions will suggest the impulse was approximately 45 psi·msec. Using Figure 1 and the limited data in Table 1 on the incidence of gut-section rupture, an impulse of approximately 36 psi·msec was estimated. Impulses in the 36 to 45 psi·msec range are consistent with the noted high levels of damage in the rats, in that the LD_{50} impulse for rats was found to be 12 psi·msec in an unpublished study previously conducted at the Lovelace Foundation. Impulses of this magnitude are also consistent with the observed 100-percent incidence of swim bladder rupture and lethality in the goldfish, in that the LD_{50} impulse was

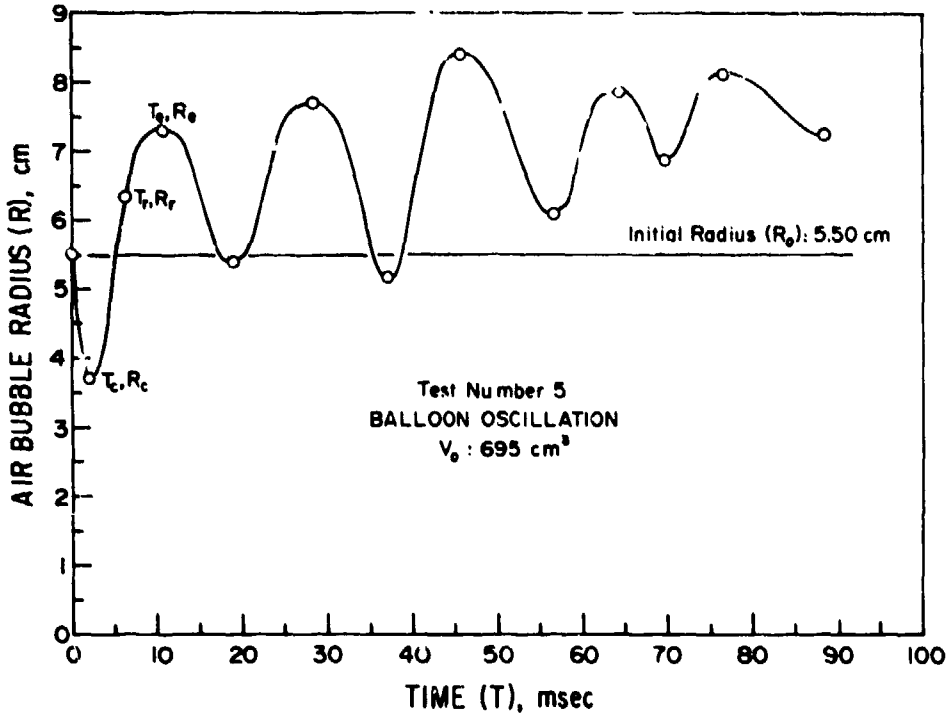

Figure 2. Air bubble radius vs time for balloon test number 5. Note that rupture (T_r, R_r) occurred on the expansion phase of the first oscillation.

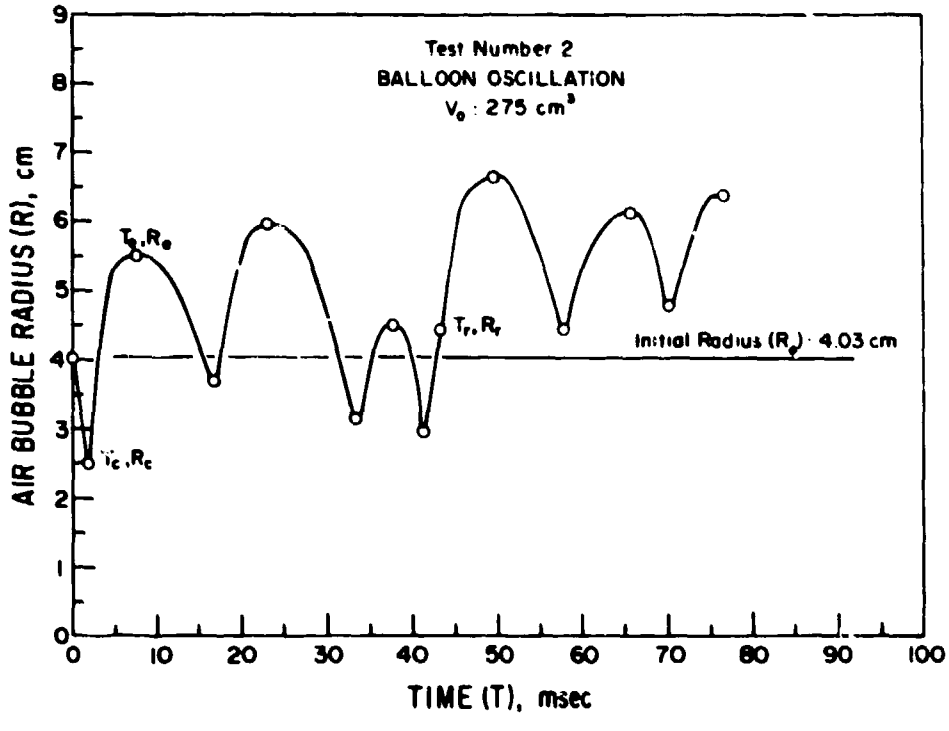

Figure 3. Air bubble radius vs time for balloon test number 2. Note that rupture (T_r, R_r,) occurred on the expansion phase of the fourth oscillation.

previously found to be from 17 to 36 psi·msec for fish of the sizes used in this study (3). Thus, the data suggest that the effective impulse in the test chamber was between 36 and 45 psi·msec, which is consistent with the predictions.

B. *Pond Tests*

1. *Injuries to Sheep*

After testing, the sheep were autopsied; they generally had moderate to extensive lung hemorrhage and multiple gut ruptures. This was to be expected because six of the seven sheep were exposed from six to eight times apiece, with each having received at least two impulses as large as 89 psi·msec.

2. *Internal Overpressures*

Usable internal overpressure vs time records were obtained on 44 of the 45 tests conducted in the pond. In general, each record exhibited a damped oscillation which was observable for as many as three overpressure peaks in the thorax and seven peaks in the abdomen. The pressure changes were relatively slow and did not have the appearance of shock waves. However, the first peak overpressure (P_c) became larger, and the time (T_c) to reach it became smaller, as the incident impulse (I) became larger.

Representative thoracic and abdominal records are shown in the left- and right-hand columns, respectively, in Figure 4. The three records in either column are arranged in order of increasing impulse. In each case, zero time corresponds to the arrival of the shock wave in free water at the slant range of the internal gauge. The following qualitative comments about the records in Figure 4 may be applied to the internal records in general.

The thoracic record in Figure 4 for an incident impulse of 22 psi·msec has a first peak overpressure of only 2 psi. Random fluctuations obscurred any subsequent peaks that may have been present. For an impulse of 67 psi·msec, a fairly sharp first peak and a lower, rounded second peak can be seen. An approximate oscillation frequency (f) of 46 cps was calculated from the spacing of these two peaks. For an impulse of 89 psi·msec, three equally spaced peaks of decreasing height indicated that the thorax was undergoing a damped oscillation of 46 cps. Note that the oscillation frequencies were the same for the latter two records which were obtained in the thorax of one animal exposed at different impulse levels.

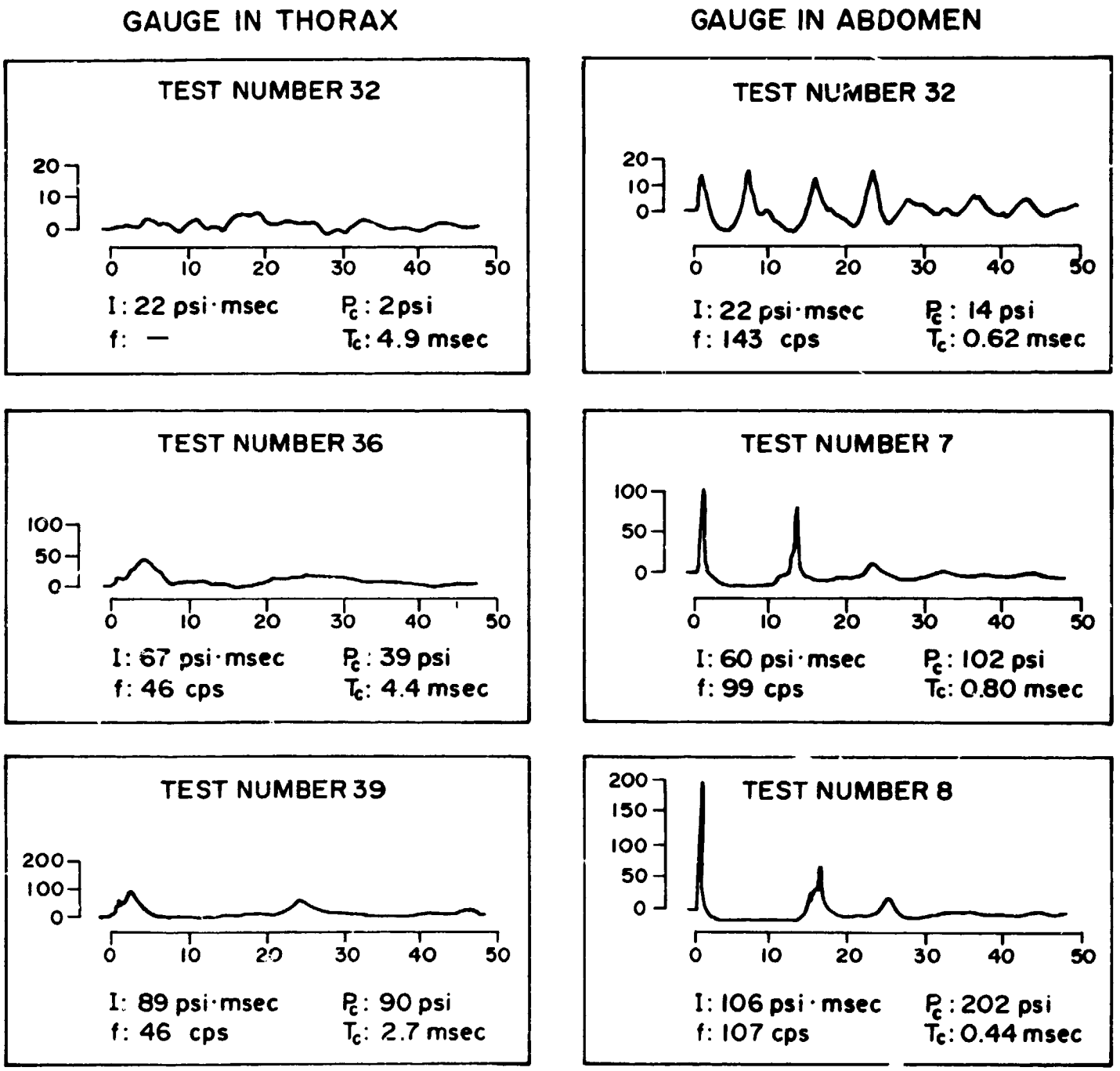

OVERPRESSURE in psi is indicated on the Vertical Scales.

TIME in msec is Indicated on the Horizontal Scales.

I : Incident Overpressure Impulse

f : Frequency of Oscillation

P_c: First Peak Overpressure

T_c: Time to First Peak Overpressure

Figure 4. Sample overpressure vs time records obtained with gauges inside sheep exposed to shock waves in water.

The abdominal record in Figure 4 for an incident impulse of 22 psi·msec has seven equally spaced peaks giving an "f" of 143 cps. Note that P_c was only 14 psi and, although the early peaks were higher than the later peaks, the decrease was relatively small and not uniform from peak to peak. This indicates that small oscillations in the abdomen are not highly damped. In contrast, the record for an impulse of 60 psi·msec (P_c of 102 psi) shows a much higher level of damping, at least for the first three oscillations. It can be seen that although the second through the fifth peaks are approximately equally spaced, the time interval between the first and second peaks is somewhat longer. The only lengthened time intervals observed in this study were between the first two peaks of abdominal records for large incident impulses. These lengthened intervals were not used in computing the oscillation frequencies. The abdominal records for tests 7 and 8 in Figure 4 were obtained with the same animal and, although the records are simlar in most respects including oscillation frequencies, the time interval between the first two peaks is longer for the larger impulse than for the smaller.

Values read from the internal overpressure records are given in Table 2. First peak overpressure, P_c, was obtained on 32 tests for the thorax and 44 tests for the abdomen. Time to P_c was also recorded. In some instances, as many as seven peaks could be read on a single record. Excluding the first peak, if no decay was apparent in two or more consecutive peaks, the overpressures were averaged and the values, thus smoothed, are also given in Table 2. Because only the first peak was measurable for low doses to the thorax, only 20 frequencies were obtained for the thorax, whereas 38 frequencies were obtained for the abdomen.

The internal overpressure records have been discussed thus far in terms of the peaks and the spacings between them. Also of interest was the first minimum overpressure, P_e, which occurred approximately midway between the first two peaks. The conditions at P_e should correspond to the conditions when the oscillating gas bubble has grown to its maximum size. One would expect the minimum overpressure to become more negative (corresponding to a larger bubble) as the incident impulse is increased, with the theoretical limit being the negative of the hydrostatic pressure, $-P_o$. For the smaller impulses to the abdomen

(e.g., see upper right-hand record in Figure 4) accurate values of P_e, falling between zero and $-P_o$, were measured from the records and listed in Table 2. For the larger impulses to the abdomen, the sensitivity of the internal gauges was set so low (in order to record the first peak overpressures) that the minimum overpressures could not be read with precision. However, within reading accuracy, the P_e's for the largest impulses to the abdomen were always approximately equal to $-P_o$, and this value was listed in Table 2. No P_e values were read for the thorax due to the large random fluctuations in the gauge records.

3. *Incident Shock Wave*

On each test in the pond, the measured incident shock wave corresponded closely to the predictions (5). The predicted values of peak overpressure, surface cut-off time, overpressure impulse and decay time constant for the incident wave are given in Table 2.

C. *Conditions at Rupture*

In the earlier studies, the incident impulse required to rupture a gut section in free water or *in vivo* was determined as a function of the volume of the enclosed air bubble (Figure 1). However, no information was obtained on the conditions at the moment of rupture. In contrast, the beginning of rupture could be seen on the motion pictures obtained in the chamber for each of the eight balloons and four excised swim bladders tested and for five of the nine gut sections which ruptured (from a total of 22 gut sections tested). The conditions at rupture are listed in Table 1.

Four of the eight balloons ruptured on the expansion phase of the first oscillation (i.e., $T_c < T_r < T_e$) at a volume greater than the initial one (i.e., $V_r > V_o$). An example is shown in Figure 2. The other four balloons ruptured during a subsequent expansion phase and, in at least two and probably three cases, the volume at rupture was larger than the initial volume but not as large as the balloon had been (and withstood) on the first oscillation. An example is shown in Figure 3. Every balloon ruptured at a volume that was smaller than the volume that the balloon could have withstood if it has been inflated slowly. Balloons rupturing on the first oscillation appeared to be approximately spherical at the moment of rupture, but those surviving the first oscillation became very distorted in shape prior to failing.

The five gut sections and four swim bladders (two being in gelatin) ruptured during the expansion phase of the first oscillation. Each of the five gut sections and two of the swim bladders ruptured at a volume that was larger than the initial one, judging from the fact that the time of rupture was significantly larger than twice the time to the first minimum volume. Gut sections which did not rupture on the first oscillation became distorted in shape during the subsequent oscillations.

In summary, for balloons, swim bladders and gut sections, most observed ruptures occurred on the expansion phase of the first oscillation at a volume larger than the initial one.

D. *Frequency of Oscillation*

1. *Objects Exposed in Chamber*

The oscillation frequencies (Table 1) measured from the films of the various objects in the test chamber are plotted in Figure 5 as a function of the initial gas volume. The lines in the figure correspond to the theory for a spherical bubble of ideal gas undergoing small polytropic changes in an ideal liquid. The two polytropic exponents considered are $\gamma = 1.4$ (adiabatic process for air) and $\gamma = 1.0$ (isothermal process). The theoretical formula (6) for the frequency, f, is

$$f = (6\pi^2 V_0)^{-1/3} (3\gamma P_0/\rho)^{1/2} \qquad (1)$$

where V_0 is the gas volume, P_0 is the hydrostatic pressure and ρ is the density of the liquid. Except for the balloons, the gas volumes listed in Table 1 were measured before the objects were submersed to a depth of 12.5 inches. The placing of the objects in the water corresponded to an increase in hydrostatic pressure with a resultant decrease in gas volume which, according to Formula 1, should have increased the oscillation frequencies about 3 percent. However, such a small change could not be detected within the scatter of the data.

Although the measured frequencies shown in Figure 5 reasonably correspond to theory for gas volumes from 0.5 to 2370 cm^3, it is not obvious that the line for $\gamma = 1.4$ (the polytropic exponent usually assumed) fits the data more

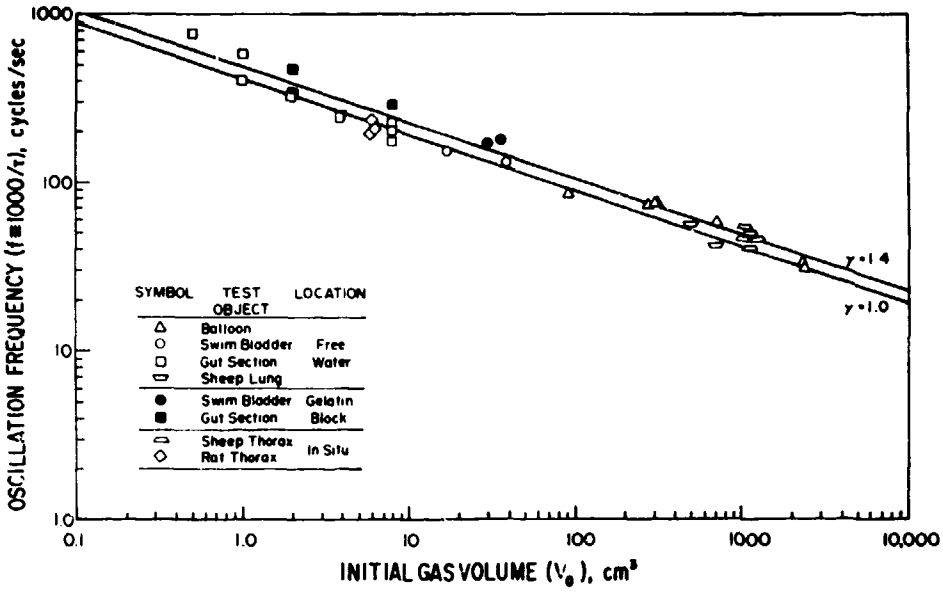

Figure 5. Oscillation frequencies of various gas-containing objects exposed to underwater blast.

satisfactorily than the line for $\gamma = 1.0$. Note that the frequencies for the swim bladders and gut sections in gelatin blocks are higher than the frequencies for the same objects in free water. Such an increase has been explained (7) by assuming a constant shear modules, μ, for the substance (in this case gelatin) surrounding the gas bubble. For that condition, 4μ would have to be added to the $3\gamma P_o$ term in Formula 1, thereby increasing the predicted frequency.

2. *Sheep Thorax and Abdomen*

The oscillation frequencies measured with the gauges inside the sheep exposed in the pond are listed in Table 2. A thoracic frequency was measured from 2 to 6 times (once per test) for each of five sheep, and an abdominal frequency was measured from 3 to 8 times (once per test) for each of six sheep. The frequencies did not seem to be a function of the incident impulse or the number of times the sheep had been tested previously. All of the frequencies measured with one gauge in one animal were within 6 percent of the geometric mean for that particular gauge and animal, except for the abdominal frequencies of two sheep (numbers 2 and 3) for which deviations as large as 16 and 19 percent were observed.

The geometric-mean thoracic frequencies for the five sheep were 41, 46, 46, 50 and 54 cps (geometric mean: 47.2 cps), and the abdominal frequencies for the six sheep were 100, 112, 123, 133, 147 and 189 cps (geometric mean: 131 cps). These frequencies did not appear to be a function of the body mass of the sheep (36 to 42 kg) or of the charge weight used (1 or 8 lb). The frequencies for the animals at a 10-ft depth did not seem to differ significantly from the corresponding frequencies for animals at a 1-ft depth. Formula 1, however, would predict that, due to increased hydrostatic pressure and decreased initial volume, the frequencies for the deep animals should have been about 25 percent higher than those for the shallow animals. That no such frequency difference was noted may be due, in part, either to the small sample size and the observed variability between animals (frequencies at both depths were not obtained for any individual sheep) or to the mechanical strength of the tissues which could have kept the hydrostatic pressure from increasing as much, and the initial volume from decreasing as much, as would have been predicted for a gas bubble in free water. In any case, it seems likely that increased frequencies would have been observed if the sheep had been tested at greater depths.

The average measured thoracic frequencies for the sheep (two at a 1-ft depth and three at a 10-ft depth) are plotted in Figure 5. All five points fall close to the line for $\gamma = 1.4$. The average measured abdominal frequencies for the sheep (three at a 1-ft depth and three at a 10-ft depth) are not plotted in Figure 5 because the initial gas volumes are unknown. Evidence will be presented later suggesting that the abdominal frequencies would also be expected to fall along the line for $\gamma = 1.4$; thus, it was possible to use the observed frequencies to estimate that the six sheep had abdominal gas volumes of 114, 83, 62, 49, 36 and 17 cm^3 (geometric mean: 51 cm^3). That the abdominal frequencies were more variable (between sheep) than the thoracic frequencies is thereby interpreted as resulting from the fact that the abdominal gas volumes were more variable (between sheep) than the thoracic gas volumes. It should be emphasized that the estimated abdominal gas volume is not necessarily all, or even most, of the gas in the abdomen, but rather corresponds to a volume of gas which is coherently oscillating in the vicinity of the abdominal gauge. The measured thoracic frequencies, however, correspond to gas volumes of the approximate size of the estimated total amount of gas in the lungs.

E. *Amplitude of Oscillation*

It has been shown experimentally that gas bubbles in various submersed objects oscillate with approximately the frequencies predicted for the limiting case of small-amplitude oscillations. For such small amplitudes, the gas pressure as well as the bubble volume and radius should undergo symmetrical oscillations (in the form of sinusoids) about their equilibrium (i.e., initial) values. However, even without damping, none of these quantities would be expected to oscillate symmetrically when the amplitudes are large. The oscillation theory, neglecting damping, is discussed in Appendix A, and computer-generated predictions are given in Table 3. The radius, volume and overpressure for the bubble at both maximum compression and maximum expansion, as well as the time to the first maximum compression, are given for 15 different incident overpressure impulses assuming a γ of either 1.4 or 1.0. These parameters were calculated in a dimensionless form by scaling them in terms of the initial radius and volume, the hydrostatic pressure and the small-amplitude oscillation period.

TABLE 3

THEORETICAL OSCILLATIONS OF A SPHERICAL BUBBLE OF IDEAL GAS

EXPOSED TO AN IMPULSIVE SHOCK WAVE IN AN IDEAL LIQUID

Specific Heat Ratio (γ)	Scaled Parameters*							
	Incident Overpressure Impulse ($I/(P_o\tau)$)	Minimum Radius (R_c/R_o)	Minimum Volume (V_c/V_o)	Maximum Overpressure (P_c/P_o)	Time to R_c, V_c, and P_c (T_c/τ)	Maximum Radius (R_e/R_o)	Maximum Volume (V_e/V_o)	Minimum Overpressure (P_e/P_o)
1.4	.01883	.9720	.9183	.1267	.2419	1.028	1.087	-.1107
	.02663	.9605	.8861	.1845	.2379	1.040	1.125	-.1524
	.05955	.9126	.7601	.4681	.2236	1.091	1.297	-.3051
	.1031	.8512	.6167	.9676	.2056	1.156	1.554	-.4607
	.1883	.7384	.4026	.2574E+1	.1732	1.294	2.164	-.6607
	.2663	.6449	.2683	.5310E+1	.1476	1.419	2.857	-.7700
	.3766	.5304	.1492	.1334E+2	.1178	1.597	4.075	-.8601
	.4294	.4830	.1127	.2026E+2	.1061	1.682	4.761	-.8875
	.4982	.4280	.07840	.3431E+2	.09317	1.792	5.759	-.9138
	.5955	.3624	.04758	.7006E+2	.07846	1.947	7.376	-.9390
	.8422	.2455	.01480	.3635E+3	.05451	2.326	12.59	-.9712
	.1235E+1	.1468	.003163	.3160E+4	.03600	2.897	24.30	-.9885
	.2382E+1	.05373	.1551E-3	.2153E+6	.01808	4.363	83.07	-.9979
	.4613E+1	.01833	.6158E-5	.1971E+8	.009254	6.718	30.32E+1	-.9997
	.8422E+1	.006766	.3098E-6	.1296E+10	.005058	10.01	10.03E+2	-.9999
1.0	.01592	.9667	.9033	.1070	.2421	1.033	1.103	-.09368
	.02251	.9529	8652	.1558	.2381	1.047	1.148	-.1290
	.05033	.8947	.7162	.3963	.2250	1.105	1.350	-.2595
	.08717	.8180	.5474	.8269	.2072	1.182	1.652	-.3947
	.1592	.6707	.3017	.2314E+1	.1736	1.331	2.358	-.5759
	.2251	.5413	.1586	.5305E+1	.1452	1.465	3.146	-.6822
	.3183	.3744	.05247	.1806E+2	.1108	1.652	4.505	-.7780
	.3629	.3040	.02810	.3458E+2	.09715	1.739	5.260	-.8099
	.4211	.2240	.01123	.8801E+2	.08229	1.852	6.348	-.8425
	.5033	.1354	.002485	.4014E+3	.06649	2.008	8.091	-.8764
	.7118	.02556	.1670E-4	.5987E+5	.04444	2.388	13.61	-.9265
	.1044E+1	.5531E-3	.1692E-9	.5911E+10	.02961	2.953	25.75	-.9612
	.2013E+1	.1880E-11	.6640E-35	.1506E+36	.01516	4.405	85.45	-.9883
	.3898E+1	.2666E-43	.1894E-130	.5280E+131	.007806	6.744	30.67E+1	-.9967
	.7118E+1	.1231E-144	.1867E-434	.5355E+435	.004272	10.03	10.08E+2	-.9990

* Parameters scaled in terms of the initial radius (R_o), initial volume (V_o), the hydrostatic pressure (P_o), and the small-amplitude oscillation period (τ) of the bubble.

1. *Objects Exposed in Chamber*

Figure 6 is a plot of the scaled first minimum (V_c/V_o) and maximum (V_e/V_o) volumes for the balloons and swim bladders exposed in the test chamber. The theoretical curves were plotted from the data in Table 3. Figure 6 suggests that the air in the balloons and swim bladders underwent adiabatic changes (i.e., $\gamma = 1.4$) during oscillation. The γ could not be determined for the other objects exposed in the chamber because accurate minimum and maximum gas volumes could not be measured from the films.

2. *Sheep Abdomen*

Figure 7 is a plot of the scaled first maximum (P_c/P_o) and minimum (P_e/P_o) overpressures for the abdomen of sheep. Points were plotted only if P_e was measurably greater than $-P_o$. The theoretical curves were plotted from the data in Table 3. Figure 7 suggests that the gas in the abdomen of each sheep underwent polytropic changes with $\gamma = 1.4$. However, four of the data points fell well to the left of the curve for $\gamma = 1.4$. Each of these four points correspond to a gauge record for which the second peak overpressure (P_{c2}) was higher than the first (P_c). When these points were replotted using P_{c2} in place of P_c, they fell close to the curve (see solid symbols in Figure 7). A similar figure could not be prepared for the sheep thorax because minimum overpressures were not readable due to the random fluctuations in the records.

F. *Parameters of First Compression*

Figures 5, 6 and 7 show that gas bubbles enclosed in various submersed objects oscillated with approximately the frequencies and amplitudes predicted for similar bubbles in free water. This does not mean, however, that an enclosed bubble's response to a given load (in this case, incident overpressure impulse) will necessarily correspond to the predictions for an air bubble in free water. In particular, it is possible that the effective impulse to a gas bubble in the abdomen of an animal is smaller than the impulse incident on the surface of the animal.

In the present study, the effective impulse to the various gas bubbles was estimated from the parameters (time and bubble volume and overpressure) at the

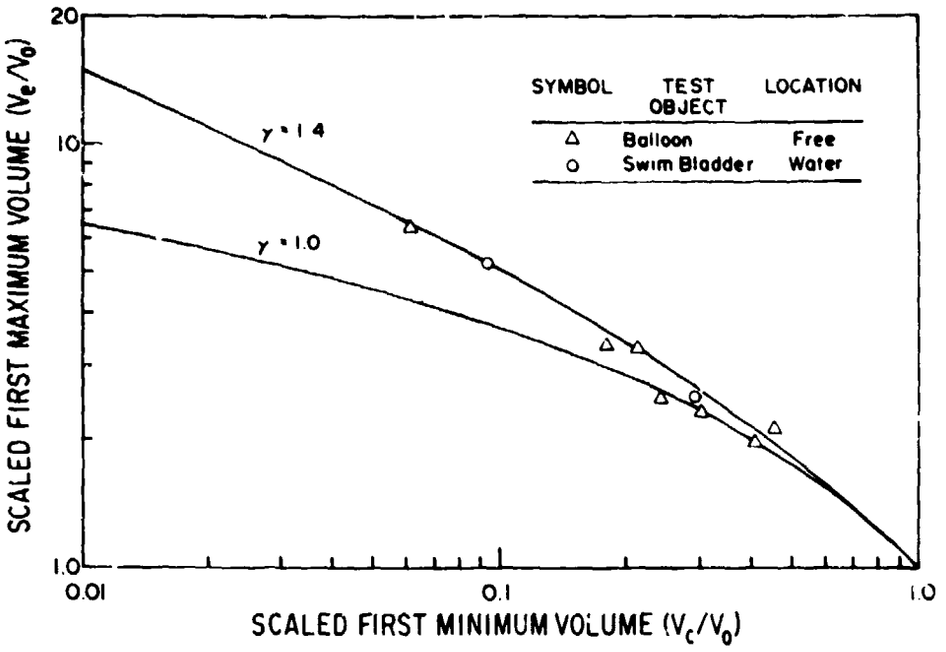

Figure 6. First maximum and minimum volumes for balloons and swim bladders.

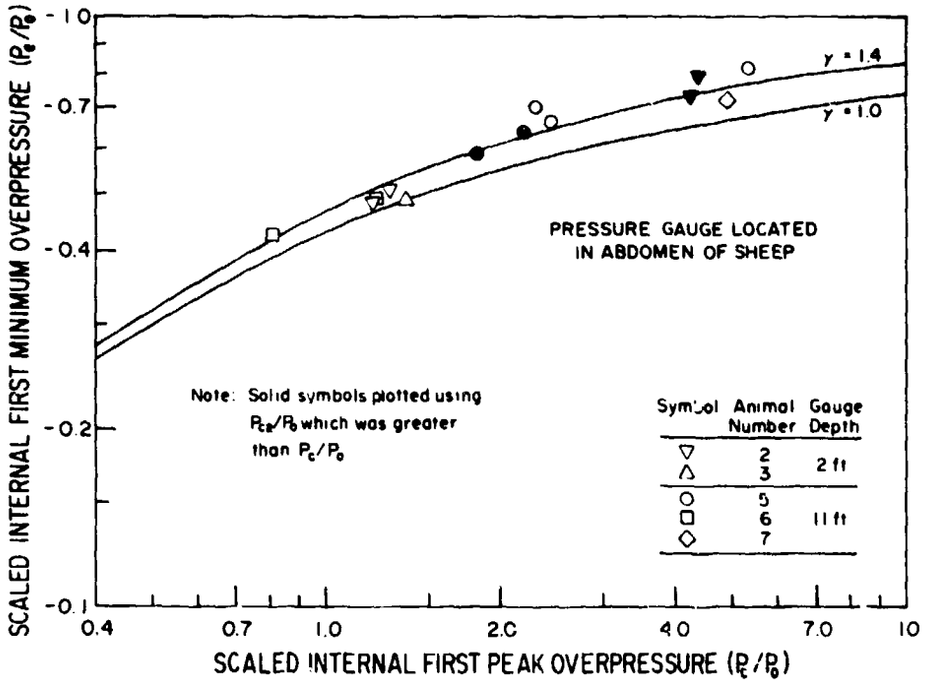

Figure 7. First maximum and minimum overpressures in a sheep abdomen.

moment of the first maximum compression. The effective impulse could also have been estimated from the parameters at the fir t maximum expansion; this was not done because (a) the presence of damping and/or mechanical strength associated with the tissues would have biased the estimation of effective impulse more for the first maximum expansion than for the first maximum compression and (b) in general, the gauges in the animals measured the maximum overpressures more accurately than the minimum overpressures.

1. *Objects Exposed in Chamber*

Figures 8, 9 and 10 show scaled first minimum volume, scaled time to first minimum volume and scaled incident overpressure impulse (based on an incident impulse of 45 psi·msec) for the various objects exposed in the test chamber. The length of the line segment associated with each data point in Figures 8 and 9 represents the discrepancy between the directly measured first minimum volume and the minimum volume calculated from the measured first maximum volume using the curve for $\gamma = 1.4$ in Figure 6. Thus, each line segment can be regarded as representing the range of uncertainty in the actual scaled first minimum volume. The curves in Figures 8, 9 and 10 were plotted from the data in Table 3.

Seven of the nine data points in Figure 8 fit the $\gamma = 1.4$ curve fairly well. The other two points suggest that the impulse was low on one swim bladder test and high on one balloon test, in both cases by approximately a factor of two. However, the data from those two tests fall close to the $\gamma = 1.4$ curves in Figures 5 and 6 suggesting that, whereas the incident impulses may have been significantly different from the assumed 45 psi·msec value, the air bubbles oscillated normally. If the two points in Figure 8 were made to fit the curve by assuming different incident impulses, (a) there would be no changes in the positions of the two corresponding points in Figure 9 and (b) the positional changes would hardly be noticeable in Figure 10 because of the large scatter in the data. The data in Figure 9 fall fairly close to the $\gamma = 1.4$ curve, whereas either curve ($\gamma = 1.4$ or $\gamma = 1.0$) fits the data reasonably well in Figure 10.

2. *Sheep Thorax (Deep)*

Figures 11, 12 and 13 show scaled first peak overpressure, scaled time to first peak overpressure and scaled incident overpressure impulse for the

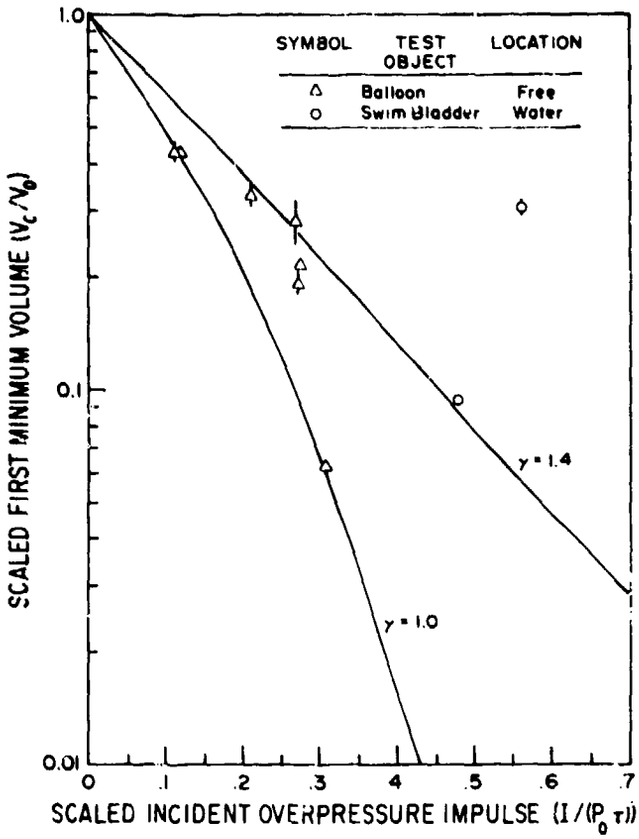

Figure 8. Incident overpressure impulse vs first minimum volume for balloons and swim bladders.

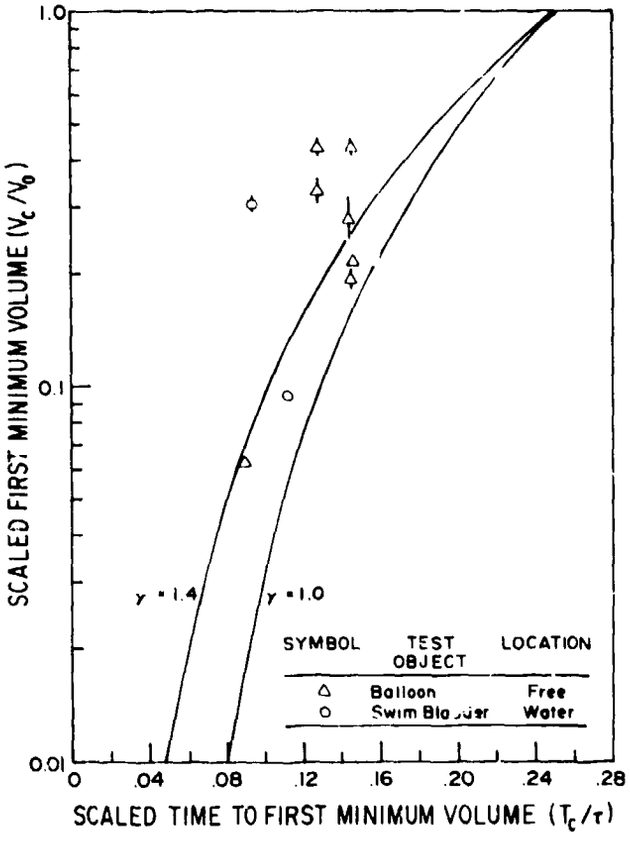

Figure 9. First minimum volume vs time to first minimum volume for balloons and swim bladders.

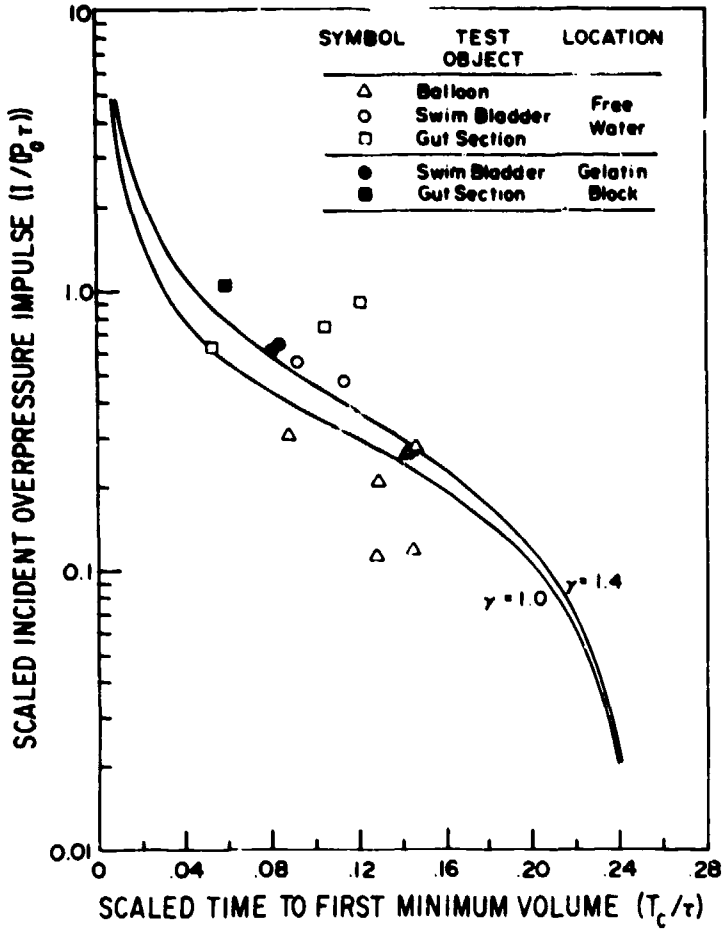

Figure 10. Incident overpressure impulse vs time to first minimum volume for balloons, swim bladders and gut sections.

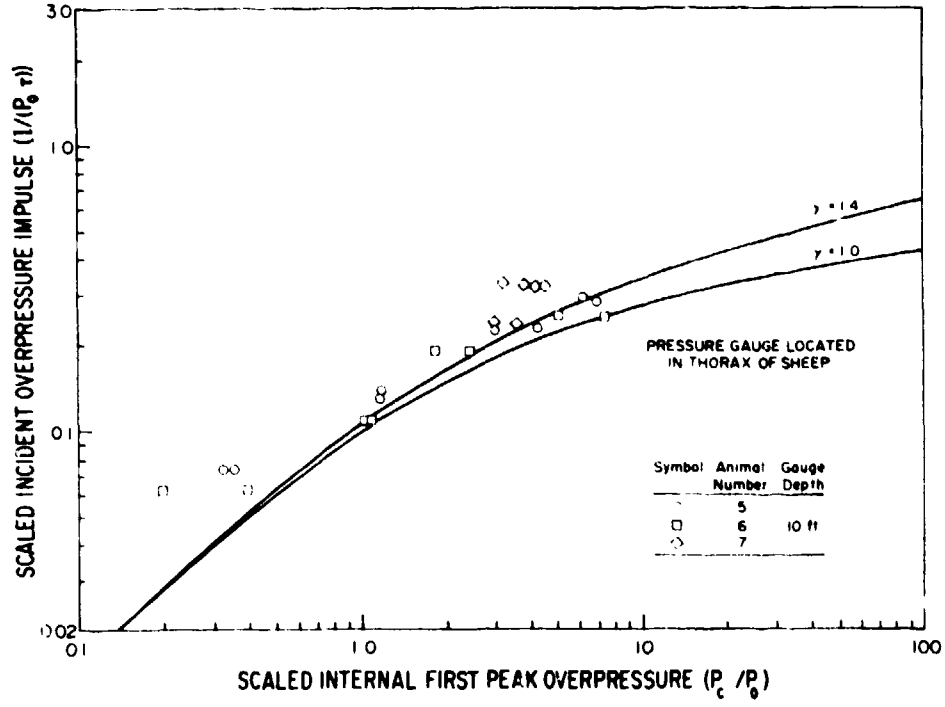

Figure 11. Incident overpressure impulse vs first peak overpressure in a sheep thorax at a 10-ft depth.

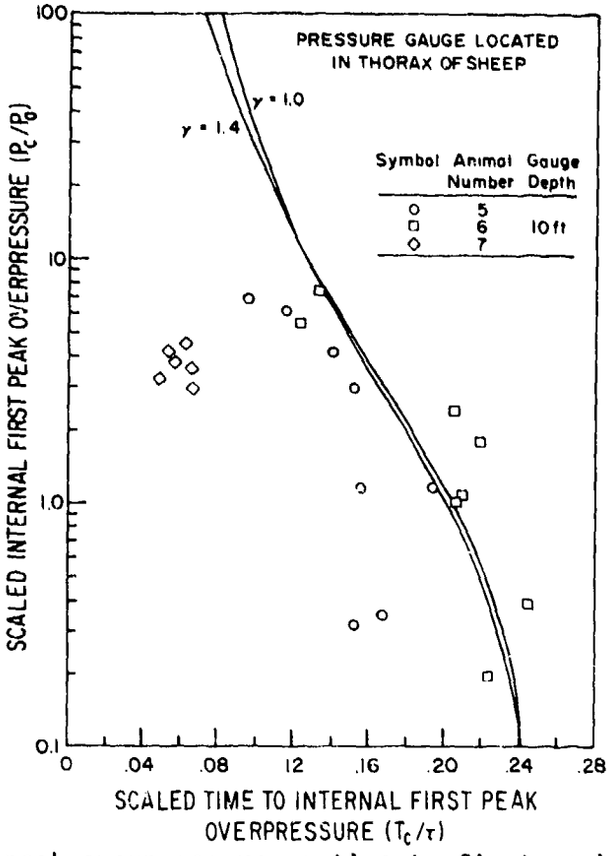

Figure 12. First peak overpressure vs time to first peak overpressure in a sheep thorax at a 10-ft depth.

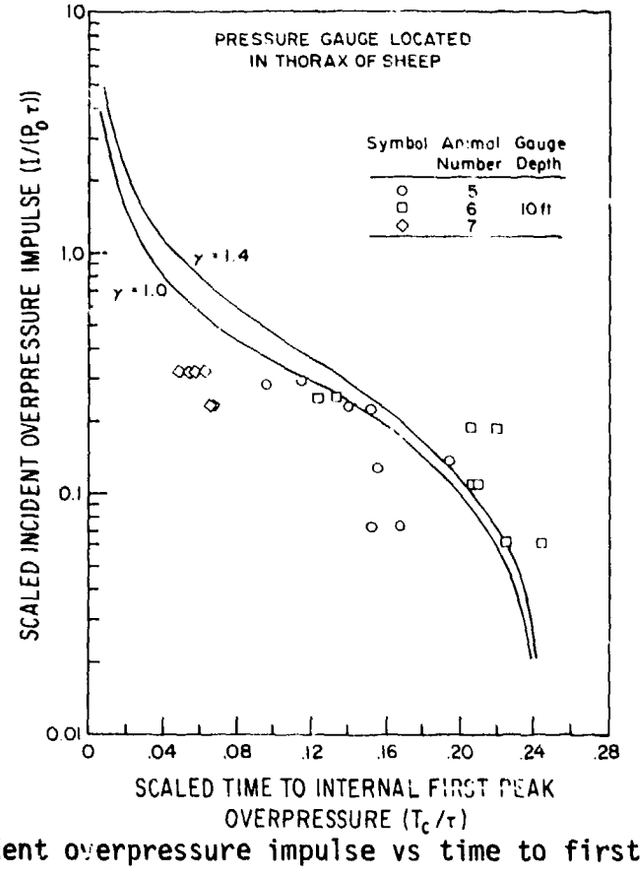

Figure 13. Incident overpressure impulse vs time to first peak overpressure in a sheep thorax at a 10-ft depth.

thorax of sheep exposed at a 10-ft depth in the test pond. The data were taken from Table 2 and the curves were drawn from the data in Table 3. The data in Figure 11 fit the $\gamma = 1.4$ curve fairly well for internal overpressures greater than P_o, whereas the measured internal overpressures less than 0.4 P_o were smaller than the values that would be predicted from the curve.

Although there is general agreement between the experimental data and the theory, determination of the appropriate value of γ from looking at Figures 12 and 13 would be difficult. Some of the scatter in these figures seems to have been caused by the variability between animals; for example, the scaled times to first peak overpressure were consistently small for animal number 7.

3. *Sheep Thorax (Shallow)*

Figures 14, 15 and 16 show the scaled parameters at the first maximum compression for the thorax of sheep exposed at a 1-ft depth. Figure 14 illustrates that the measured first peak overpressures were lower than predicted at all incident impulse levels. Further, Figures 15 and 16 indicate that each peak overpressure was significantly lower than the value that would have been predicted from the measured time required to reach that peak, even though the times were close to the predictions based on incident impulse. The large discrepancies between theory and the thoracic data for a 1-ft depth (as opposed to the relatively good agreement for a 10-ft depth) may have been due, at least in part, to the fact that the lungs, being relatively large and near the surface, did not receive a uniform load. In particular, the tops of the lungs which were near the surface level of the pond received a much smaller impulse than the incident impulse at a depth of 1 ft (approximately the mid-depth of the lungs) which was used to plot the data in Figures 14 and 16. Two other possible explanations for overpressures' measured inside the animals being lower than theory are discussed in the following section.

4. *Sheep Abdomen*

Figures 17, 18 and 19 show the scaled parameters at the first maximum compression for the abdomen of sheep exposed at either a 2- or an 11-ft depth. The data for the two depths were combined because no systematic differences were noted. The measured first peak overpressures were smaller than predicted (Figure 17), with the discrepancy increasing with the dose. Figures 18 and 19

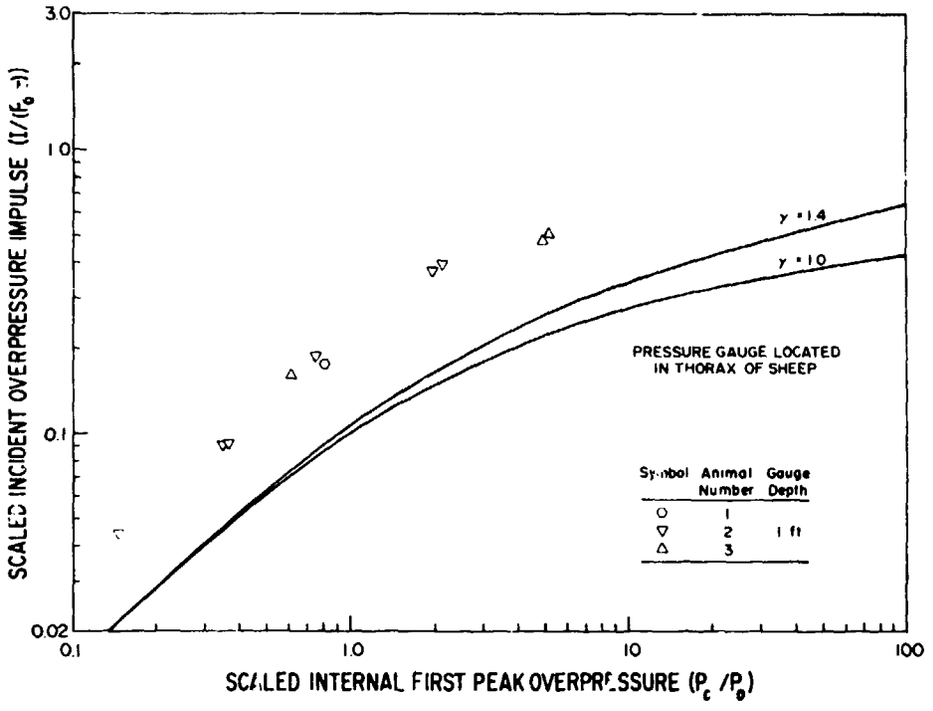

Figure 14. Incident overpressure impulse vs first peak overpressure in a sheep thorax at a 1-ft depth.

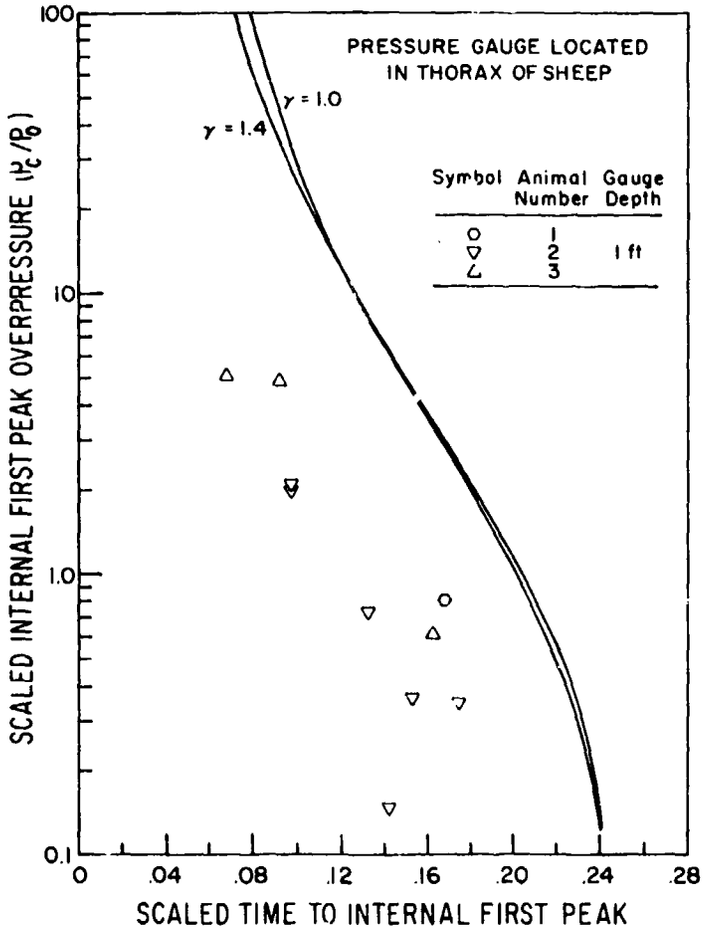

Figure 15. First peak overpressure vs time to first peak overpressure in a sheep thorax at a 1-ft depth.

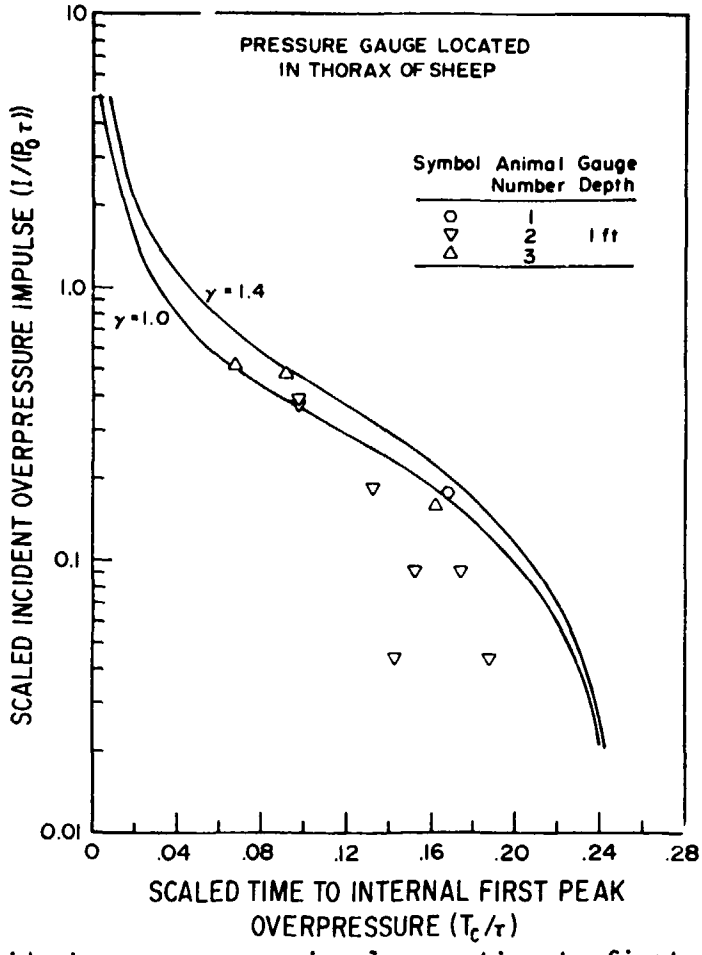

Figure 16. Incident overpressure impulse vs time to first peak overpressure in a sheep thorax at a 1-ft depth.

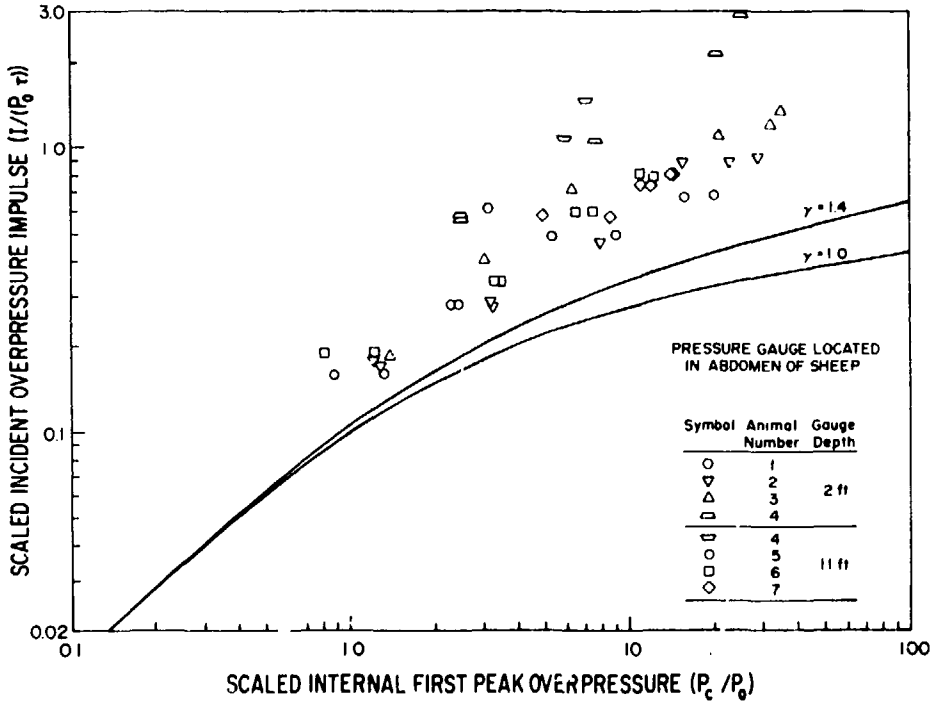

Figure 17. Incident overpressure impulse vs first peak overpressure in a sheep abdomen.

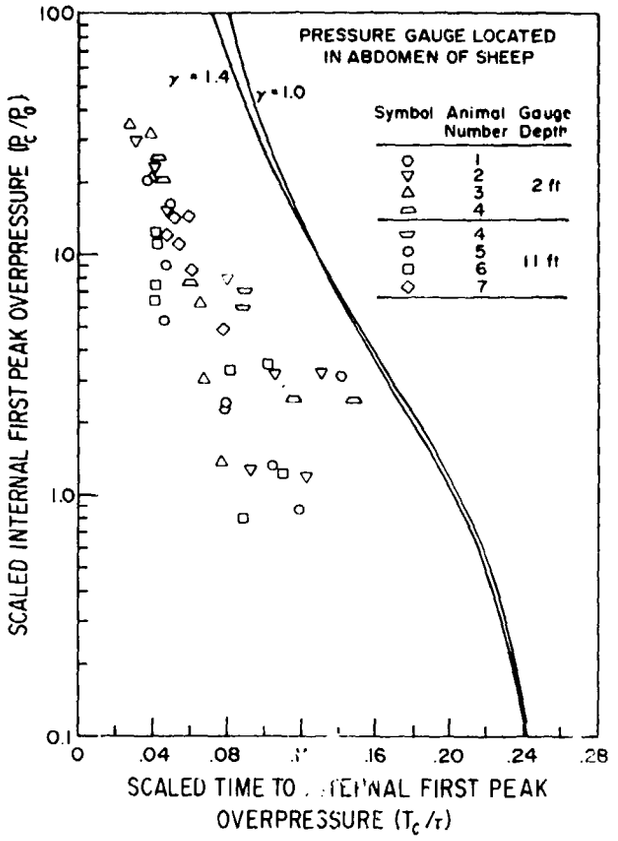

Figure 18. First peak overpressure vs time to first peak overpressure in a sheep abdomen.

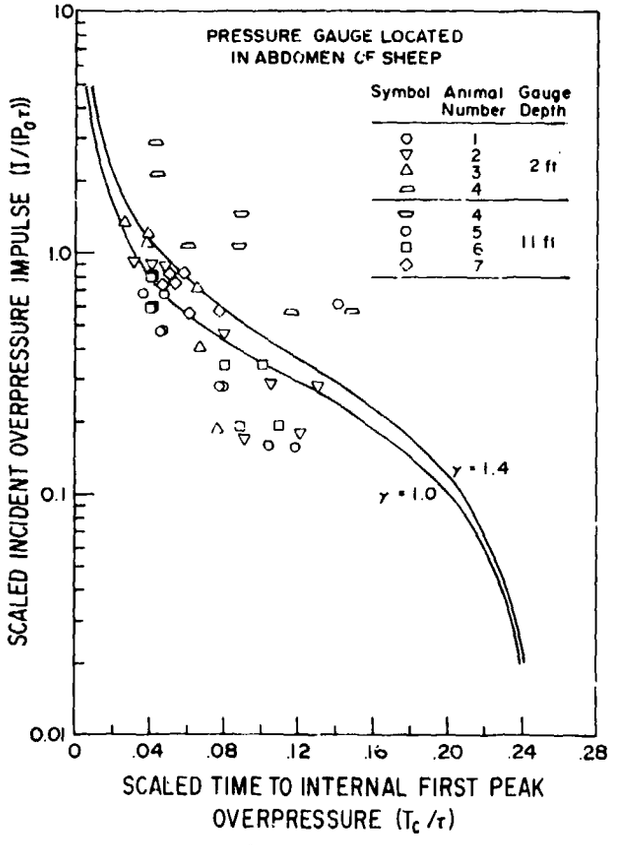

Figure 19. Incident overpressure impulse vs time to first peak overpressure in a sheep abdomen.

indicate that, similar to what was found for the thorax at a 1-ft depth, each first peak overpressure in the abdomen was significantly lower than the value that would have been predicted from the measured time required to reach that peak, even though the times were close to the predictions based on incident impulse.

The reduced overpressures in the abdomen are probably not the result of nonuniform loading, which was suggested as a possible explanation for the reduced overpressures in the thoraces exposed at a depth of 1 ft. The loading should have been considerably more uniform on the abdomen than on the thorax for the shallow exposures due to the gas pockets' in the abdomen having a greater depth (~ 2 ft) and smaller volumes (17 to 114 cm^3 estimated) than the corresponding values (1 ft and ~ 1100 cm^3) for the thorax. At least two alternative explanations seem possible:

a. The effective dose in the abdomen was smaller than the incident dose because the wave encountered bones, inhomogenous tissues and possibly other gas pockets prior to reaching the gas pocket whose oscillations were recorded with the gauge; or

b. The gas pocket in the abdomen oscillated as predicted from the incident impulse, but the gauge measuring that oscillation was in such a position that it was not acted upon by the total overpressure developed in the gas itself.

The first explanation could account for the fact that the impulse required to rupture a gut section inside a sheep is larger than the impulse required to rupture a similar section in free water. However, the discrepancy between theory and the data in Figure 18, as well as the fair agreement in Figure 19, could both qualitatively be accounted for by the second explanation. Without further experimentation, the matter probably cannot be resolved completely.

G. *Damping*

For the reasons previously discussed (page 14), a quantitative measure of the damping rates could not be obtained in a straight-forward manner from the films of the oscillations of the gas-containing objects exposed in the test chamber. However, the records from the gauges inside the sheep did provide some information on damping. Maximum overpressures were measurable for as many

as the first seven oscillations on some of the records (Table 2). These data suggest that the larger the peak overpressure, the larger the decay from one oscillation to the next.

H. *Injury Predictions*

Much of the information in this report could be useful in predicting injury levels for untested experimental geometries. For example, consider the thoracic injuries to sheep exposed to impulsive underwater shock waves while breathing pressurized air at depths of greater than 10 ft. The agreement between data and theory shown in Figures 11, 12 and 13 indicates that a spherical air bubble in free water can be used as a model to describe the first maximum compression of the thorax of a sheep exposed to an impulsive load at a depth of 10 ft. The model may be expected to apply at greater depths as well. Although the oscillation frequencies were also consistent with the predictions (Figure 5), damping which is neglected in the model, would cause the measured overpressures to deviate from the predictions at times beyond the first maximum compression. Nonetheless, because rupturing, when observed, usually occurred during the first expansion at a larger-than-initial volume, it is probably not unreasonable to use the predicted first maximum volume to estimate the severity of lung hemorrhage.

If the exposure depth of a sheep breathing pressurized air was increased, the hydrostatic pressure would become larger but the (initial) gaseous lung volume would remain constant. The maximum volume during the first oscillation would also be expected to remain constant as the exposure depth was increased if the incident impulse varied as the hydrostatic pressure multiplied by the small-amplitude oscillation period (scaled parameters, Table 3). According to Formula 1, the small amplitude oscillation period (the reciprical of frequency) would vary as the reciprical of the square root of the hydrostatic pressure. Thus, the maximum gaseous lung volume would be independent of the depth of exposure if the incident impulse varied as the square root of the hydrostatic pressure. If this interpretation of the data is correct, the severity of lung hemorrhage in personnel using scuba gear at various depths below 10 ft should be approximately constant if each diver received an impulsive load which was proportional to the square root of the hydrostatic pressure at his depth. A similar relationship has been derived for impulsive shock waves producing lethality in animals exposed to airblast at various ambient pressures (8).

References 1 and 2 contain experimental data expressing severity of lung hemorrhage as a function of incident overpressure impulse for sheep exposed to impulsive shock waves at a depth of 10 ft. If similar data were available for greater depths, it would be possible to test the indicated hydrostatic-pressure scaling relationship.

REFERENCES

1. Richmond, D. R., J. T. Yelverton and E. R. Fletcher, "Far-Field Underwater-Blast Injuries Produced by Small Charges," Topical Report DNA 3081T, Director, Defense Nuclear Agency, Washington, D. C., July 1, 1973.

2. Yelverton, J. T., D. R. Richmond, E. R. Fletcher and R. K. Jones, "Safe Distances from Underwater Explosions for Mammals and Birds," Topical Report DNA 3114T, Director, Defense Nuclear Agency, Washington, D. C., July 13, 1973.

3. Yelverton, J. T., D. R. Richmond, W. Hicks, K. Saunders and E. R. Fletcher, "The Relationship Between Fish Size and Their Response to Underwater Blast," Topical Report DNA 3677T, Director, Defense Nuclear Agency, Washington, D. C., June 18, 1975.

4. Bowen, I. G., A. Holladay, E. R. Fletcher, D. R. Richmond and C. S. White, "A Fluid-Mechanical Model of the Thoraco-Abdominal System with Applications to Blast Biology," Technical Progress Report DASA-1675, Director, Defense Nuclear Agency, Washington, D. C., June 14, 1965.

5. Christian, E. A. and J. B. Gaspin, "Swimmer Safe Standoffs from Underwater Explosions," Technical Report NOLX 80, Naval Surface Weapons Center (formerly Naval Ordnance Laboratory), White Oak, Silver Spring, MD, July 1, 1974.

6. Kennard, E. H., "Radial Motion of Water Surrounding a Sphere of Gas in Relation to Pressure Waves," in A Compendium of British and American Reports, Vol. II, pp. 182-226, Office of Naval Research, Department of the Navy, Washington, D. C., 1950.

7. Andreeva, I. B., "Scattering of Sound by Air Bladders of Fish in Deep Sound-Scattering Ocean Layers," Soviet Physics-Acoustics, 10(1): 17-20, July-September 1964.

8. Bowen, I. G., E. R. Fletcher, D. R. Richmond, F. G. Hirsch and C. S. White, "Biophysical Mechanisms and Scaling Procedures Applicable in Assessing Responses of the Thorax Energized by Air-Blast Overpressures or by Nonpenetrating Missiles," Ann. N. Y. Acad. Sci., 152 (Art. 1): 122-146, October 28, 1968.

APPENDIX

A. *Derivation of Theoretical Equations*

Reference 6 contains a theoretical description of the oscillations of a spherical gas bubble in an incompressible fluid. For this reason, only a brief derivation of the equations used in this study will be given.

Consider a spherical bubble of an ideal gas centered at a depth, D, in an ideal liquid of density, ρ. Assume that the equilibrium radius, R_o, of the bubble is small compared to D, which in turn is small compared to the depth and breadth of the liquid. For these conditions the boundaries of the liquid, except for the surface, can be ignored and, for relatively short time intervals, the upward migration of the bubble can also be neglected. If P_o is the hydrostatic pressure at the depth of the bubble, then $P_o - g\rho D$ is the atmospheric pressure at the surface, where g is the acceleration of gravity. Assume that the bubble, while at rest, is subjected to a uniform impulsive load, I, which instantaneously gives the bubble's surface a radial velocity, $(dR/dT)_o$, whose magnitude depends on I as described in Reference 6:

$$(dR/dT)_o = -I/(\rho R_o) \tag{A1}$$

The bubble, having been set in motion by the impulsive load, will start to oscillate. Neglecting damping, and assuming that the bubble gas undergoes polytropic changes, the small-amplitude period of oscillation, τ, will be, according to Reference 6,

$$\tau = 2\pi R_o[\rho/(3\gamma P_o)]^{1/2} \tag{A2}$$

Where γ is the polytropic exponent. The only two polytropic exponents we will consider are $\gamma = 1.4$ (adiabatic process for air) and $\gamma = 1.0$ (isothermal process).

Having neglected damping, the total energy in the oscillating system should be conserved such that at any time, T, after the impulse was applied, the following would be true: (the kinetic energy of the liquid) plus (the work done on the bubble gas) plus (the work done on the atmospheric gas) plus (the change in the potential energy of the liquid) equals (the initial kinetic energy of the

liquid). Substituting the appropriate mathematical expression for each of the energy terms, while preserving their order, gives

$$2\pi\rho(dR/dT)^2 R^3 + (5/2) P_0V_0[(V/V_0)^{-2/5} - 1]$$

$$+ (P_0-g\rho D)(V-V_0) + g\rho D(V-V_0) = 2\pi R_0 I^2/\rho \qquad (A3, \gamma = 1.4)$$

$$2\pi\rho(dR/dT)^2 R^3 - P_0V_0 \ln (V/V_0)$$

$$+ (P_0 - g\rho D)(V-V_0) + g\rho D(V-V_0) = 2\pi R_0 I^2/\rho \qquad (A3, \gamma = 1.0)$$

where V_0 is the initial volume of the bubble, and R and V are the radius and volume, respectively, of the bubble at time, T. Note that Equation A3 is given in two forms corresponding to an assumed λ of either 1.4 or 1.0 for the changes in the bubble gas. Equation A3 can be put in a dimensionless form by using the parameters $J \equiv R/R_0$ and $K \equiv T/\tau$ to give

$$(10/7)\pi^2[I/(P_0\tau)]^2 = (63/40)\pi^{-2}(dJ/dK)^2J^3$$

$$+ (5/2)J^{-6/5} + J^3 - 7/2 \qquad (A4, \gamma = 1.4)$$

$$2\pi^2[I/(P_0\tau)]^2 = (9/8)\pi^{-2}(dJ/dK)^2J^3$$

$$- 3 \ln(J) + J^3 - 1 \qquad (A4, \gamma = 1.0)$$

When J has either a maximum or minimum value, dJ/dK equals zero and Equation A4 becomes

$$(10/7)\pi^2[I/(P_o\tau)]^2 = (5/2)J^{-6/5} + J^3 - 7/2 \qquad (A5,\ \gamma = 1.4)$$

$$2\pi^2[I/(P_o\tau)]^2 = -3\ \ln(J) + J^3 - 1 \qquad (A5,\ \gamma = 1.0)$$

For any value of $I/(P_o\tau)$, there are two values of J (one greater than 1.0 and the other less than 1.0) satisfying Equation A5. The equation could not be solved explicitly for J, so the solutions were obtained with an electronic computer using iterative techniques. The computed maximum and minimum J values (labeled R_e/R_o and R_c/R_o, respectively) are given (Table 3) for various values of $I/(P_o\tau)$. The scaled maximum and minimum volumes and overpressures in the table were computed directly from the J values and the appropriate value of γ.

The scaled time (T_c/τ) to the minimum radius can be found by rearranging Equation A4 to give

$$dK = -\pi^{-1}\ (63/40)^{1/2}\ \{(10/7)\pi^2\ [I/(P_o\tau)]^2 J^{-3} - (5/2)J^{-21/5} - 1 + (7/2)J^{-3}\}^{-1/2} dJ \qquad (A6,\ \gamma = 1.4)$$

$$dK = -\pi^{-1}\ (9/8)^{1/2}\{2\pi^2[I/(P_o\tau)]^2\ J^{-3} + 3J^{-3}\ \ln(J) - 1 + J^{-3}\}^{-1/2}\ dJ \qquad (A6,\ \gamma = 1.0)$$

Integrating the left-hand side of Equation A6 from zero to T_c/τ and the right-hand side from 1.0 to R_c/R_o yields

$$T_c/\tau = -\pi^{-1} (63/40)^{1/2} \int_1^{R_c/R_o} \{(10/7)\pi^2[I/(P_o\tau)]^2 J^{-3} - (5/2) J^{-21/5} - 1 + (7/2) J^{-3}\}^{-1/2} dJ \qquad (A7, \gamma = 1.4)$$

$$T_c/\tau = -\pi^{-1} (9/8)^{1/2} \int_1^{R_c/R_o} \{2\pi^2 [I/(P_o\tau)]^2 J^{-3} + 3J^{-3} \ln(J) - 1 + J^{-3}\}^{-1/2} dJ \qquad (A7, \gamma = 1.0)$$

For any value of $I/(P_o\tau)$, Equation A5 can be used to obtain the value of R_c/R_o, and these two values can be substituted into Equation A7 to compute T_c/τ. However, the integral in Equation A7 could not be evaluated in closed form, and therefore the solutions given in Table 3 were obtained with an electronic computer using numerical integration techniques.

DISTRIBUTION

Office of Naval Research Biological & Medical Sciences Division
Distribution List for Technical Reports and/or Reprints

Number of Copies	
(12)	Administrator, Defense Documentation Center Cameron Station Alexandria, Virginia 22314
(6)	Director, Naval Research Laboratory Attention: Technical Information Division Code 2027 Washington, D. C. 20375
(6)	Code 102IP (ORNL DOC) Office of Naval Research 800 N. Quincy Street Arlington, Virginia 22217
(3)	Physiology Program Office of Naval Research, Code 441 800 N. Quincy Street Arlington, Virginia 22217
(1)	Commanding Officer Naval Medical Research and Development Command National Naval Medical Center Bethesda, Maryland 20014
(1)	Technical Reference Library Naval Medical Research Institute National Naval Medical Center Bethesda, Maryland 20014
(1)	Office of Naval Research Branch Office 495 Summer Street Boston, Massachusetts 02210
(1)	Office of Naval Research Branch Office 536 South Clark Street Chicago, Illinois 60605
(1)	Office of Naval Research Branch Office 1030 East Green Street Pasadena, California 91106

(1) Office of Naval Research
Contract Administrator for Southeastern Area
2110 G Street, NW
Washington, D. C. 20037

(1) Assistant Chief for Technology
Office of Naval Research (Code 200)
800 N. Quincy Street
Arlington, Virginia 22217

(1) Donald J. Freeman, MAJ, MI
Operations Officer, U. S. Army Science
and Technology Center, Far East Office
APO San Francisco 96328

(1) Director
National Library of Medicine
8600 Wisconsin Avenue
Bethesda, Maryland 20014

(1) Commanding Officer
Naval Air Development Center
Attention: Crew Systems Department
Warminster, Pennsylvania 18974

(1) Scientific Library
Naval Aerospace Medical Research Institute
Naval Aerospace Medical Center
Pensacola, Florida 32512

(1) Commander
Army Research Office, Durham
Box CM
Duke Station
Durham, North Carolina 27706

(1) Director, Life Sciences Division
Air Force Office of Scientific Research
1400 Wilson Boulevard
Arlington, Virginia 22209

(1) Commanding General
Army Medical Research & Development Command
Forrestal Building
Washington, D. C. 20314

(1) G. Max Irving
ONR Resident Representative
University of Arizona
Room 421, Space Sciences Building
Tucson, Arizona 85721

(1) ONR Scientific Liaison Group
American Embassy - Room A-407
APO San Francisco 96503

Office of Naval Research Physiology Program
Distribution List for Hyperbaric Physiology Reports

Number of Copies

(1) Head
Submarine and Diving Medicine Division
Code 41
Naval Medical Research & Development Command
National Naval Medical Center
Bethesda, Maryland 20014

(1) Naval Medical Research Institute
National Naval Medical Center
Bethesda, Maryland 20014
ATTN: Diving Physiology

(1) Officer in Charge
Submarine Medical Research Laboratory
Naval Submarine Base, New London
Groton, Connecticut 06542

(1) Medical Officer
Naval Coastal Systems Laboratory
Panama City, Florida 32401

(1) Officer in Charge
Naval Experimental Diving Unit
Naval Coastal Systems Laboratory
Panama City, Florida 32401

(1) Commanding Officer
Naval School of Diving and Salvage
Building 214
Washington Navy Yard
Washington, D. C. 20374

(1) Medical Officer
Submarine Development, Group I
Fleet Post Office
San Diego, California 92132

(1) Dr. Thomas K. Akers
Project Manager
Man-in-the-Sea
Department of Physiology and Pharmacology
The University of North Dakota
Grand Forks, North Dakota 58201

(1) Dr. Peter B. Bennett
Professor, Anesthesiology and
Biomedical Engineering
Department of Anesthesiology
Duke University Medical Center
Durham, North Carolina 27710

(1) Dr. James D. Blankenship
The Marine Biomedical Institute
The University of Texas Medical Branch
at Galveston
260 University Boulevard
Galveston, Texas 77550

(1) Dr. Ralph W. Brauer
Director, Wrightsville Marine Biomedical Lab
University of North Carolina
7205 Wrightsville Avenue
Wilmington, North Carolina 28401

(1) Dr. Chryssanthos Chryssanthou
Associate Director of Research
Beth Israel Medical Center
New York, New York 10003

(1) Dr. E. N. Cohen
Professor of Anesthesia
Stanford University School of Medicine
Stanford, California 94305

(1) Dr. Morris Faiman
Associate Professor of Pharmacology
and Toxicology
The University of Kansas
Lawrence, Kansas 66044

(1) Dr. J. C. Farmer
Department of Surgery
Duke University
Durham, North Carolina 27710

(1) Dr. William P. Fife
Department of Biology
Texas A&M University
College of Science
College Station, Texas 77483

(1) Dr. E. R. Fletcher
Lovelace Foundation for Medical Education
and Research
P. O. Box 5890
Albuquerque, New Mexico 87115

(1) Dr. William R. Galey
Assistant Professor, Department of Physiology
University of New Mexico School of Medicine
915 Stanford Drive, NE
Albuquerque, New Mexico 87131

(1) Dr. J. D. Hackney
Research Physiologist
Rancho Los Amigos Hospital
12826 Hawthorn Street
Downey, California 90242

(1) Dr. B. A. Hills
Chief, Hyperbaric Physiology
Section, Marine Biomedical Institute
University of Texas Medical Branch
Galveston, Texas 77550

(1) Drs. W. J. Johnson & K. E. Money
Department of Otolaryngology
University of Toronto
92 College Street
Toronto, Ontario M5S 1A1
Canada

(1) Dr. Eric P. Kindwall
Director
Department of Hyperbaric Medicine
St. Luke's Hospital
2900 W. Oklahoma Avenue
Milwaukee, Wisconsin 53215

(1) Dr. C. J. Lambertsen
Director
Institute for Environmental Medicine
University of Pennsylvania
Medical Center
Philadelphia, Pennsylvania 19104

(1) Dr. J. G. McCormick
Director, Otological Laboratories
Department of Surgery
Bowman Gray School of Medicine
Wake Forest University
Winston-Salem, North Carolina 27103

(1) Dr. Stanley A. Mendoza
Associate Professor of Pediatrics
Department of Pediatrics
School of Medicine
University of California, San Diego
P. O. Box 109
La Jolla, California 92037

(1) Dr. John Miller
Department of Anesthesiology
Duke University Medical Center
Durham, North Carolina 27710

(1) Dr. Josef M. Miller
Assistant Professor
Departments of Otolaryngology and
Physiology and Biophysics
School of Medicine
University of Washington
Seattle, Washington 98195

(1) Dr. Keith W. Miller
Department of Pharmacology
Harvard Medical School
25 Shattuck Street
Boston, Massachusetts 02115

(1) Dr. R. D. Paegle, Research Consultant
Department of Anesthesiology
New York University Medical Center
550 First Avenue
New York, New York 10016

(1) Dr. V. Popovic
Professor, Department of Physiology
Division of Basic Health Sciences
Emory University
Atlanta, Georgia 30322

(1) Dr. Hermann Rahn
Professor of Physiology
Department of Physiology
Schools of Medicine and Dentistry
State University of New York at Buffalo
Buffalo, New York 14214

(1) Dr. John Salzano
Associate Professor
Department of Physiology and Pharmacology
Duke University Medical Center
Durham, North Carolina 27710

(1) Dr. Aaron P. Sanders
Professor and Director
Division of Radiobiology
Duke University Medical Center
Durham, North Carolina 27710

(1) Dr. Christopher Schatte
Instructor
Departments of Physiology, Biophysics
and Biochemistry
Colorado State University
Fort Collins, Colorado 80521

(1) Dr. C. W. Sem-Jacobsen
Director, EEG Laboratory
Gaustad Sykehus
Vinderen, Oslo 3
Norway

(1) Dr. Charles W. Shilling
Undersea Medical Society, Inc.
9650 Rockville Pike
Bethesda, Maryland 20014

(1) Dr. E. B. Smith
Physical Chemistry Laboratory
Oxford University
South Parks Road
Oxford OX1 3OZ, England

(1) Dr. Kent H. Smith
Director, Diving Physiology and
Hyperbaric Research
Virginia Mason Research Center
1000 Seneca Street
Seattle, Washington 98101

(1) Dr. Merrill P. Spencer
Director
Institute of Applied Physiology & Medicine
1700 East Cherry Street - Suite 105
Seattle, Washington 98122

(1) Dr. W. G. Thomas
University of North Carolina
School of Medicine
Chapel Hill, North Carolina 27514

(1) Dr. Paul Webb
Principal Associate
Webb Associates
Box 308
Yellow Springs, Ohio 45387

(1) Dr. H. S. Weiss
Professor
Department of Physiology
Ohio State University
4196 Medical Sciences Building
333 West Tenth Avenue
Columbus, Ohio 43210

(1) Dr. C. H. Wells
Assistant Professor
Department of Physiology
University of Texas Medical Branch
9th and Strand
Galveston, Texas 77550

(1) Dr. Eugene H. Wissler
Associate Dean for Academic Affairs
University of Texas at Austin
College of Engineering
Austin, Texas 78712